Global and Planetary Change 236 (2024) 104436

Contents lists available at ScienceDirect

Global and Planetary Change

journal homepage: www.elsevier.com/locate/gloplacha

An updated chronostratigraphic framework for the Cenozoic sediments of southeast margin of the Tibetan Plateau: Implications for regional tectonics

Shihu Li [a], Robert A. Spicer [b,c,d], Tao Su [e], Zhekun Zhou [b], Chenglong Deng [a,*]

[a] State Key Laboratory of Lithospheric Evolution, Institute of Geology and Geophysics, Chinese Academy of Sciences, Beijing 100029, China
[b] CAS Key Laboratory of Tropical Forest Ecology, Xishuangbanna Tropical Botanical Garden, Chinese Academy of Sciences, Mengla 666303, China
[c] School of Environment, Earth and Ecosystem Sciences, The Open University, Milton Keynes MK7 6AA, UK
[d] State Key Laboratory of Tibetan Plateau Earth System, Resources and Environment (TPESRE), Institute of Tibetan Plateau, Chinese Academy of Sciences, Beijing 100101, China
[e] State Key Laboratory of Oil and Gas Reservoir Geology and Exploitation & Institute of Sedimentary Geology, Chengdu University of Technology, Chengdu 610059, China

ARTICLE INFO

Editor: Sun Jimin

Keywords:
Chronostratigraphy
Southeast margin of Tibetan Plateau
Cenozoic
Uplift
Sedimentary basin

ABSTRACT

As one of the most important accommodation zones during the India-Asia collision, the southeast margin of the Tibetan Plateau (SEMTP) is characterized by many large-scale strike-slip faults, a regional low-relief relict that has been deeply incised by several continental scale rivers that originate from central Tibet, and numerous plant and vertebrate fossil biotas residing in Cenozoic sedimentary basins. Therefore, the SEMTP not only provides a meaningful constraint on the geodynamic evolution of the Tibetan Plateau, but also serves as an exemplar to understand the various interactions among surface uplift, drainage network reorganization, climate change, and biodiversity. Precise dating of Cenozoic sediments in the basins of the SEMTP is crucial for understanding these processes. Previously, the geochronologic framework of Cenozoic sediments in the SEMTP largely relied on fossils and regional stratigraphic correlations, which often involved circular reasoning and large uncertainties. In the past two decades, high-resolution magnetostratigraphy, detrital zircon geochronology, and isotopic dating of interbedded tephra layers have been carried out on SEMTP Cenozoic sedimentary basins in Yunnan and eastern Xizang provinces, SW China. Using these new data, we build a revised chronostratigraphic framework for Cenozoic sediments in SEMTP, and use this updated temporal framework to contextualize regional tectonics and climate change. The new chronostratigraphic framework shows that (1) many of the "Neogene" sedimentary basins based on plant fossils and regional lithostratigraphic correlation in the SEMTP were actually formed in the late Eocene and early Oligocene; (2) most of the Paleogene sedimentary successions in the SEMTP ended at the late Eocene-early Oligocene and were unconformably overlaid by Middle-Late Miocene sediments. Oligocene-Early Miocene sediments are often regionally absent. Sedimentary structures within the basin successions show that Paleogene basins were generally formed in compressional settings while the Late Miocene basins were mostly developed in extensional settings. The new chronostratigraphic framework, together with analyses of sedimentary basin structures, suggests that the SEMTP began to experience crustal shortening early in the India-Asia collision (~50 Ma), producing Paleogene sedimentary basins and giving rise to the subsequent widespread surface uplift and regional erosion in the Oligocene-Middle Miocene. Tectonic inversion from compression to extension since the Middle Miocene precludes significant uplift of the SEMTP after this time, which may be related to geodynamic changes in the evolution of the Tibetan Plateau.

1. Introduction

The Tibetan Plateau, the largest and highest orographic feature in the world, is largely the product of ongoing indentation of India into Asia beginning in the early Cenozoic. The Cenozoic development of the Tibetan Plateau has not only significantly modified the topography of Asia, but also atmospheric circulation, which in turn resulted in climate changes across Asia, and even the entire globe (e.g., Molnar et al., 1993; Wu et al., 2022). Moreover, Tibetan region mountain systems have driven the biodiversity changes in East Asia, making Tibetan Plateau one

* Corresponding author.
E-mail address: cldeng@mail.iggcas.ac.cn (C. Deng).

https://doi.org/10.1016/j.gloplacha.2024.104436
Received 30 September 2023; Received in revised form 5 February 2024; Accepted 9 April 2024
Available online 10 April 2024
0921-8181/

of Earth's most important biodiversity hotspots (Favre et al., 2015; Su et al., 2019; Spicer et al., 2020; Li et al., 2021; Zhou et al., 2022). Therefore, the Tibetan region represents one of the best natural laboratories for studying the geodynamics of continental-continental collision and the coupled evolution between lithosphere, atmosphere, and biosphere.

The southeast margin of the Tibetan Plateau (SEMTP), between the Sagaing and Xianshuihe-Xiaojiang-Red River faults, and southeast of the Eastern Himalaya Syntaxis (Fig. 1), is one of the key areas to understanding the tectonic evolution of the Tibetan Plateau. This area is dissected by several large-scale strike-slip faults (Fig. 1), e.g., Ailao Shan-Red River, Sagaing-Gaoligong, and Xianshuihe-Xiaojiang, which were regarded as boundary faults to accommodate the rigid-block extrusion of Indochina ("extrusion model", e.g., Tapponnier et al., 1982) or as a manifestation of north-striking right-lateral shear to accommodate the N-S shortening and clockwise rotation of eastern Tibet ("crustal shortening model", England and Molnar, 1990). In addition, the SEMTP is characterized by high elevation but low relief, where the elevation decreases southeastward gradually from the interior of Tibetan Plateau to the marginal sea (Clark et al., 2006; Liu-Zeng et al., 2008). This has been attributed to the southeastward flow of the Tibet's thickened lower crust ("lower crustal flow model", e.g., Royden et al., 1997). Moreover, this typical topography enables the warm and moist air of the Indian Monsoon to move into the interior of the Tibetan Plateau, and is related to the development of the three large continental scale rivers, i.e., the Yangtze, Mekong, and Salween (Fig. 1). The deeply incised uplifted mountains, especially the Hengduan Mountains, and the warm and wet climate, mean that the SEMTP is a cradle and refuge for both animals and plants, and a hotspot of biodiversity in the context of continuous cooling and aridification in western China during the Late Cenozoic (Xing and Ree, 2017; Ding et al., 2020; Spicer et al., 2020).

Long successions in sedimentary basins of SEMTP preserve a rich archive for understanding surface uplift, fault activity, climate change, drainage networks and biodiversity evolution, and are therefore crucial to understanding the tectonic evolution of the Tibetan Plateau and its impact on climate and biotic change. Several Cenozoic terrestrial sedimentary basins are well developed in eastern Xizang and Yunnan provinces (Fig. 2), and these basins have been widely used to constrain the timing of regional surface uplift, fault activity, drainage network evolution, climate change and the establishment of biodiversity (Leloup et al., 1995; Wang et al., 1998; Clark et al., 2004; Schoenbohm et al., 2006a; Yan et al., 2012; Su et al., 2019; Li et al., 2020a; Fang et al., 2021). However, previously, most of the Cenozoic basins in the SEMTP lacked absolute age constraints, and the ages of these basins have mainly relied on biostratigraphic and lithostratigraphic correlations, often based on limited plant fossils (including pollen), which have inherent ambiguities when used as age tie points to constrain the tectonic/climate events(Hoke, 2018).

In the past two decades, many magnetostratigraphic studies, pinned with isotopic dating on interbedded tuffs and biostratigraphic studies, have been conducted on the Cenozoic basins in the SEMTP (e.g., Zhu et al., 2005, 2008a; Ji et al., 2013; Li et al., 2013, 2015, 2020a, 2020b,

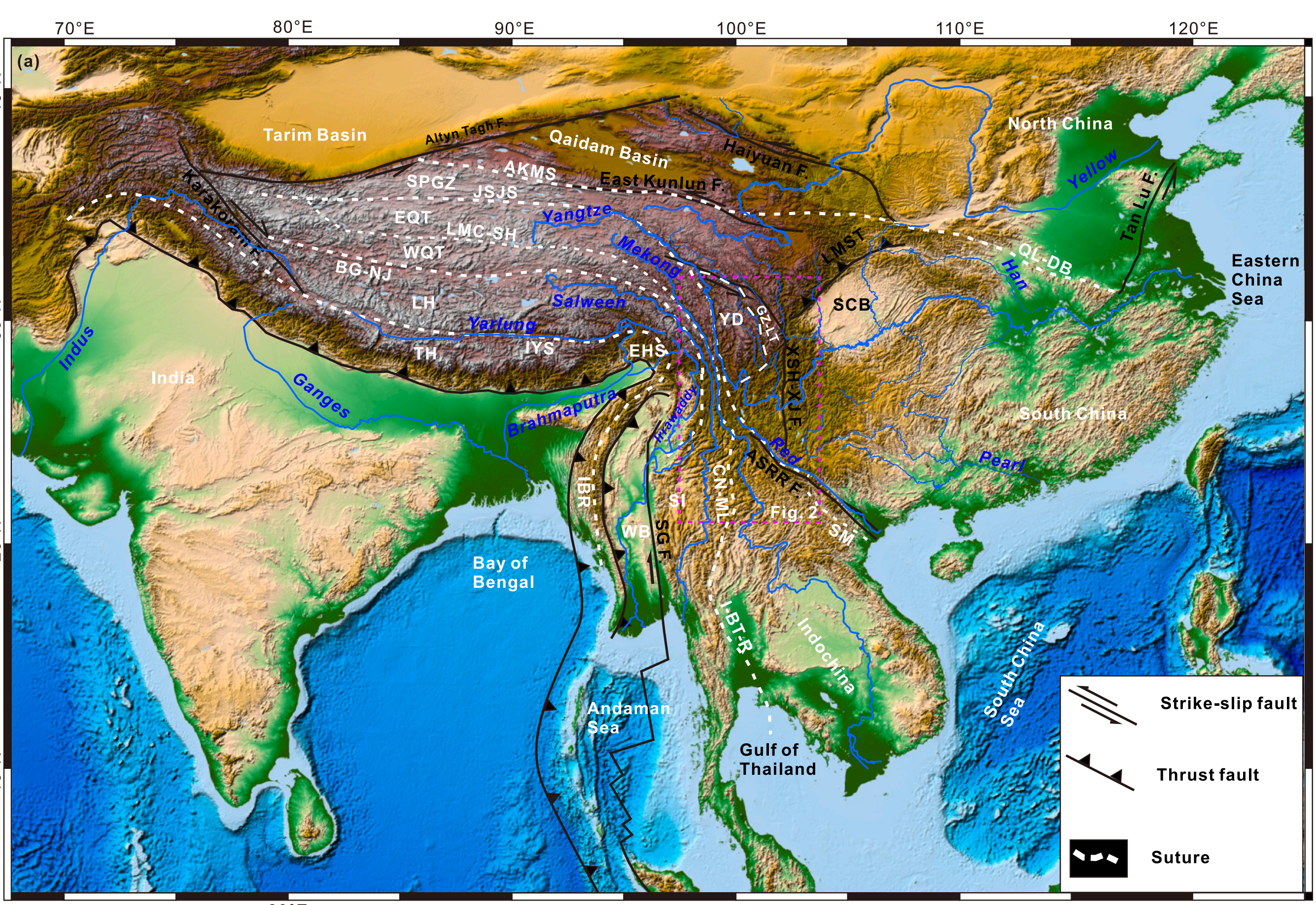

Fig. 1. Map illustrating major geological terranes, sutures, faults, and major fluvial drainages in East and SE Asia. Abbreviations: TH: Tethyan Himalaya, LH: Lhasa terrane, E/WQT: East/West Qiangtang terrane, SPGZ: Songpan-Ganzi terrane, YD: Yidun Arc, WB: West Burma Block, SI: Sibumasu terrane. AKMS: Anyimaqin-Kunlun-Muztagh suture, QL-DB: Qinling-Dabie, JSJS: Jinshajiang suture, LMC-SH: Longmuco-Shuanghu suture, BG-NJ: Bangonghu-Nujiang suture, IYS: Indus-Yarlung suture, CN-ML: Changning-Menglian suture, I-BT-R: Inthanon-Bentong-Raub suture, SM: Songma suture, GZLT: Ganzi-Litang suture. EHS: Eastern Himalaya Syntaxis, IBR: Indo-Burman Ranges, SGF: Sagaing Fault, LMST: Longmen Shan Thrust Fault, SCB: Sichuan Basin.

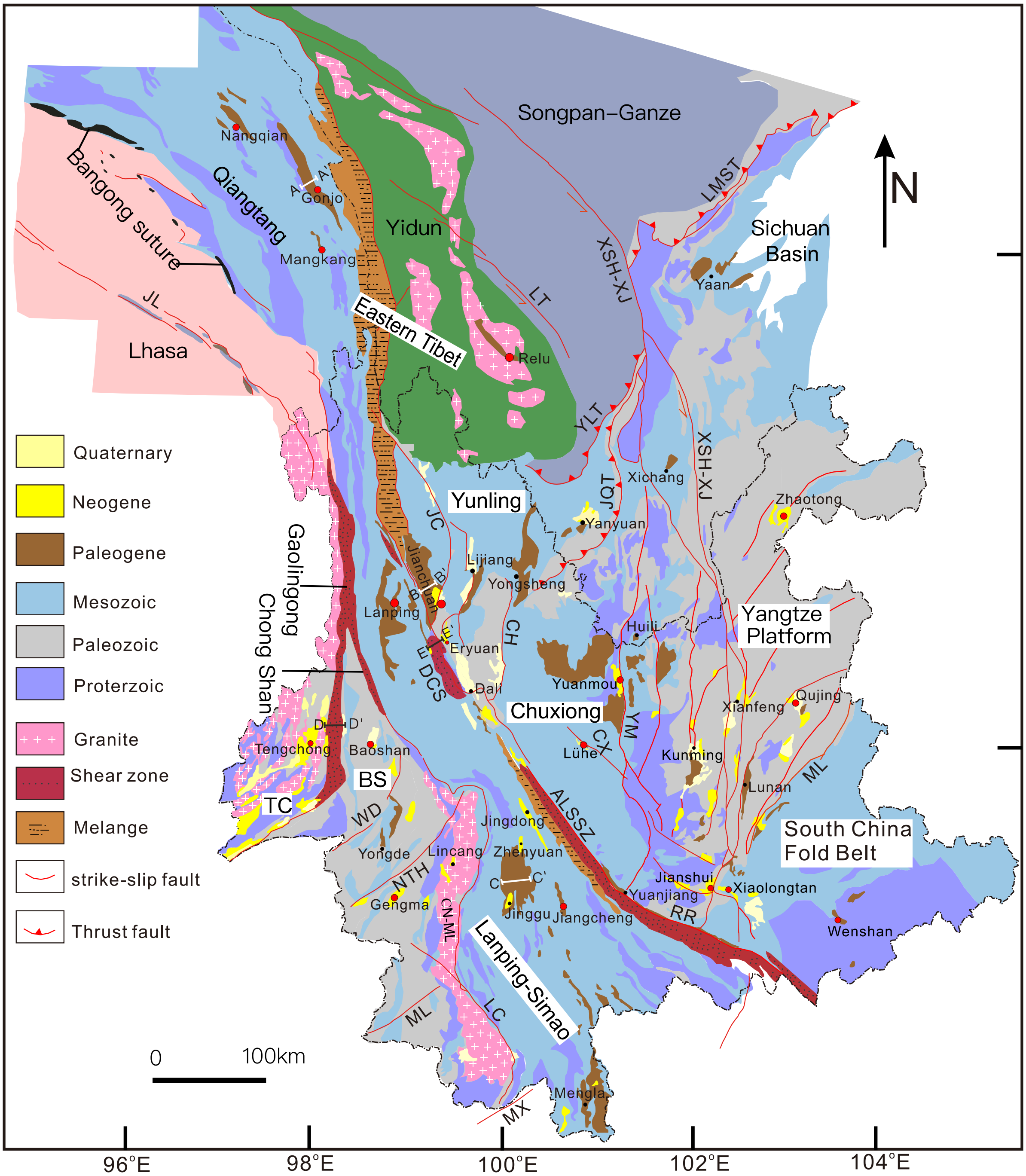

Fig. 2. Tectonic map of the southeast margin of the Tibetan Plateau showing the main stratigraphic units, Cenozoic sedimentary basins, and fault systems. The red dots refer to the basins that have reliable new age constraints. Abbreviations: XSH-XJ: Xianshuihe-Xiaojiang fault, LT: Litang fault, YLT: Yalong thrust fault, JQT: Jinhe-Qinghe thrust fault, CH: Chenghai fault, JC: Jianchuan fault, JL: Jiali fault, DCS: Diancang Shan, ALSSZ: Ailao Shan shear zone, RR: Red River fault, ML: Mile fault, MX: Mengxing fault, ML: Menglian fault, LC: Lingcang fault, NTH: Nantinghe fault, WD: Wanding fault, BS: Baoshan terrane, TC: Tengchong terrane. The others are the same as in Fig. 1. (For interpretation of the references to colour in this figure legend, the reader is referred to the web version of this article.)

2020c; Gourbet et al., 2017; Linnemann et al., 2018; Su et al., 2019; Xiong et al., 2020; Fang et al., 2021; Tian et al., 2021; He et al., 2022). These new ages have greatly improved age constraints on the sedimentary successions in these basins, thereby providing an opportunity to build an updated chronostratigraphic framework for the Cenozoic basins in the SEMTP. In this study, we first conduct a comprehensive review on the stratigraphy and updated age constraints for the Cenozoic sedimentary basins in southeastern Xizang and Yunnan provinces; we then build an updated chronostratigraphic framework for the Cenozoic sedimentary basins in the SEMTP. Next, we summarize the sedimentary signatures of typical basins, their contained records of paleoelevation and low-temperature thermochronological data, and briefly discuss the tectonic/climate implications within this new chronostratigraphic framework.

2. Geological settings

2.1. Regional tectonic background of Tibet and East Asia

The Tibetan Plateau and East Asia are composed of a series of mosaic blocks, including North China, South China, Tarim, Songpan-Ganzi, Yidun arc, east/west (or north/south) Qiangtang, Lhasa, Sibumasu and Indochina (Fig. 1), which amalgamated progressively during the closure of the Paleo- and Neo-Tethys Oceans in the Mesozoic and Cenozoic (e.g., Wu et al., 2020; Zhu et al., 2021). The Qiangtang/ Sibumasu and Indochina blocks collided with northeastern Tibet-North China-South China in the Early-Late Triassic by closing the Paleo-Tethys Ocean (e.g., Wu et al., 2020), as today represented by the Jinshajiang and Longmuco-Shuanghu sutures in central Tibet (Wang et al., 2000), the Ailao Shan-Songma and Changning-Menglian belts in southwestern China, and the Bentong-Raub suture in Thailand and Malaysia (Metcalfe, 1996, Fig. 1). The Lhasa Block collided with the Qiangtang in Late Jurassic-Early Cretaceous by closing the north branch of Neo-Tethys (or Meso-Tethys), as now represented by the Bangong-Nujiang suture in central Tibet (e.g., Li et al., 2019, Fig. 1). The final collision between India and Lhasa (Eurasia) along the Yarlung-Tsangpo suture in early Cenozoic evidenced the demise of Neo-Tethys and the start of processes that led to the formation of the Tibetan Plateau.

The SEMTP in this study includes part of the east Qiangtang, the Yidun arc, the Chuandian terrane which is separated from the South China Block by the Xianshuihe-Xiaojiang fault, the Lanping-Simao terrane, the Baoshan terrane, and the Tengchong terrane (Fig. 2).

2.2. Cenozoic tectonic activity in the southeast margin of the Tibetan Plateau

One of the main tectonic features of the SEMTP is the presence of large-scale strike slip faults, which can be categorized into two groups: ductile shear zones and brittle faults.

The ductile shear zones include the Ailao Shan-Red River shear zone, the Chongshan shear zone, and the Gaoligong shear zone (Fig. 2), which were generally formed in the early Cenozoic (~35–17 Ma) to accommodate the large magnitude southeastward extrusion of Indochina and Sibumasu blocks (Tapponnier et al., 1982; Leloup et al., 1995; Bertrand et al., 2001; Searle et al., 2007). Estimates of displacement along the Ailao Shan-Red River shear zone range from 1500 km to ~500 km in the northwest of the fault (Leloup et al., 1995; Chung et al., 1997), but no more than ~250 km at the southeastern part of the fault (Fyhn et al., 2009; Mazur et al., 2012). The decreasing offset along the Ailao Shan-Red River shear zone, together with the varied vertical axis rotations of fault-bounded blocks in the Indochina Block as determined by paleomagnetic data, led Li et al. (2017a) to propose an internal deformation model for the extrusion of Indochina, i.e., the extrusion of Indochina is as large as 600 km along the northwestern of the Ailao Shan-Red River shear zone, but only 250 km in the southeastern end, while the remaining ~350 km extrusion was accommodated by rotation and deformation within NW Indochina. There are no field-based estimates of displacement within the Chongshan and Gaoligong shear zones, although Pellegrino et al. (2018) estimate 230–290 km dextral displacement along the Gaoligong shear zone based on palaeomagnetically determined vertical axis rotation of fault rocks.

The main brittle faults are the Xianshuihe-Xiaojiang, Red River, and Sagaing faults (Yunnan Bureau of Geology and Mineral Resources (YBGMR), 1990, Fig. 1). The Xianshuihe-Xiaojiang fault separates the strongly deformed southeastern Tibet margin from the stable South China Block and was previously regarded as a left-lateral strike-slip fault that initiated at ~13 Ma (Li et al., 2015; Roger et al., 1995; Wang et al., 2008b) and accumulated a total displacement of ~80–100 km (Wang et al., 1998). However, recent structural geology and thermochronological studies suggest that this fault has accommodated significant shortening and exhumation since at least 35 Ma (Zhang et al., 2022).

The Red River fault, along the front of the Ailao Shan shear zone (Fig. 2), has been inverted as a dextral fault since the Late Miocene (Leloup et al., 1995; Li et al., 2013; Schoenbohm et al., 2006b) and has accommodated a ~ 40 km right-lateral displacement (Schoenbohm et al., 2006b; Wang et al., 1998).

The N-S oriented Sagaing fault accommodates part of the northward motion of India Plate (Fig. 1). It initiated at either 4–5 Ma (Raju et al., 2004), ~11 Ma (Curray, 2005) or as early as ~27.5 Ma (Morley and Arboit, 2019), with a total displacement of 100–150 km (Bertrand and Rangin, 2003), 250 km (Zaw, 1990), or 460–530 km (Van Hinsbergen et al., 2011), to as large as 1100 km or more (Mitchell, 1993; Mitchell et al., 2012). Moreover, a set of small NE-SW striking faults have developed in the southwest of the Ailao Shan-Red River shear zone, such as the Wanding, Nanting, and Mengxing faults (Fig. 2). These faults were initiated no later than the Late Miocene, with tens of kilometers of displacement (Lacassin et al., 1998; Socquet and Pubellier, 2005; Wang and Burchfiel, 1997; Wang et al., 1998).

3. Traditional and new age constraints on Cenozoic stratigraphy in the southeast margin of the Tibetan Plateau

Because the SEMTP comprises a collage of crustal fragments (see Section 2.1), which were strongly deformed during the Cenozoic by the India and Eurasia collision, the correlation of Cenozoic stratigraphy among different fragments in the SEMTP has always been difficult. Therefore, when discussing the Cenozoic stratigraphic age framework, the SEMTP is generally divided into several stratigraphic units based on their geological background. These include eastern Tibet, the Yunling collage, the Chuxiong basin, the Yangzi Platform, the South China fold belt, the Lanping-Simao fold belt, and the Baoshan and Tengchong terranes (YBGMR, 1990; Wang et al., 1998, Fig. 2). Below we will introduce the traditional and new age constraints on the Cenozoic sediments for each unit.

3.1. Cenozoic stratigraphy in eastern Tibet

Eastern Tibet consists of part of the north Qiangtang terrane and the Yidun arc. Cenozoic sediments accumulated in the Nangqian, Gonjo, Mangkang, and Relu (also named as Mula) basins (Fig. 2). In the Nangqian and Gonjo basins, the sediments are divided into Gonjo and Ranmugou formations from old to young (Bureau of Geology and Mineral Resources of Xizang (BGMR Xizang), 1993, Fig. 3). The Gonjo Formation is dominated by red-colored mudstones, sandstones, and conglomerates (Studnicki-Gizbert et al., 2008), and is characterized by abundant gypsum (Studnicki-Gizbert et al., 2008; Wang et al., 2022b, Fig. 4a). In the Nangqian Basin, marlites and limestones interbedded with volcanic rocks are also widespread in the red beds (Horton et al., 2002; Spurlin et al., 2005; Zhang et al., 2020). The Ranmugou Formation comprises red-colored sandstones, conglomerates, and rare carbonaceous shales, carbonates and red mudstones (Studnicki-Gizbert et al., 2008; Tang et al., 2017; Li et al., 2020a, Fig. 4b). Based on plant fossils, originally identified as *Palibinia* sp., *Alstonia* sp., *Salix* sp., *Carpinus* sp., and *Ephedripites* sp. from the Gonjo and Ranmugou formations, a Paleocene-Eocene age was assigned to the Gonjo and Ranmugou formations in the geological map of Xizang Province (BGMR Xizang, 1993). However, the volcanic rocks in the upper Ranmugou Formation from the northern Gonjo Basin yielded an age of ~43 Ma based on $^{40}Ar/^{39}Ar$ and U—Pb zircon dating methods (Studnicki-Gizbert et al., 2008; Tang et al., 2017). Although Xiao et al. (2021) argued that in the central Gonjo Basin deposition ceased at ~50 Ma, a high-resolution magnetostratigraphy study from the central part of the Gonjo Basin suggested that deposition took place between 69 and 41.5 Ma (Li et al., 2020a, Fig. 5n). This age is consistent with the isotopic dating of volcanic rocks in the upper Ranmugou Formation from both the northern (Studnicki-Gizbert et al., 2008; Tang et al., 2017) and southern parts of the basin (Xiong et al., 2020), both of which show that the Gonjo Basin deposition ended at around 40 Ma. Moreover, a detailed palynological study in the upper Ranmugou Formation from the southern part of the Gonjo Basin also yielded an age of ~48–44 Ma for the upper Ranmugou Formation (Wang et al., 2022b). Therefore, it is reliable to conclude that the Gonjo Basin started forming in the Late Cretaceous and development continued until

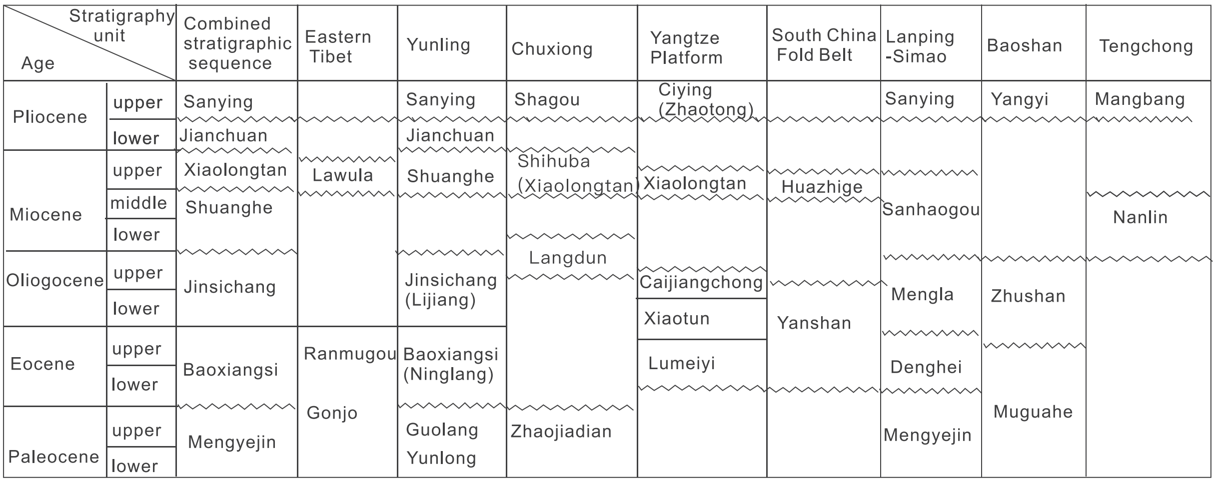

Fig. 3. Traditional Cenozoic stratigraphy framework in the southeast margin of the Tibetan Plateau, modified from YBGMR (1990) and BGMR Xizang (1993).

the late middle Eocene. Magnetostratigraphy, together with zircon U—Pb ages of interbedded volcanic rocks from Nangqian Basin (Spurlin et al., 2005), shows that the Cenozoic Nangqian Basin succession was deposited between 52 and 35 Ma (Zhang et al., 2020, Fig. 5q).

In the Relu Basin, sediments are divided into the Changzong and Relu formations, which are dominated by thick matrix-supported conglomerates at the bottom, interbedded conglomerates and sandstones at the middle, and conglomerates at the top (Bureau of Geology and Mineral Resources of Sichuan (BGMR Sichuan), 1991; Jackson et al., 2018, Fig. 4b). Notably, eolian dune deposits are preserved in the lower parts of the successions in both the Gonjo and Relu basins (Xiong et al., 2020; He et al., 2022). Plant fossils, such as "*Eucalyptus" reluensis*, *Palibinia* sp., and "*Pistacia*" sp., as well as gastropods like *Pakistania sinensis* and *Australorbis* sp., have been reported from the Relu Formation (Guo, 1986), which was assigned an Eocene age in the geological map of Sichuan Province (BGMR Sichuan, 1991). Based on a weighted mean age of the youngest detrital zircon U—Pb ages from the Relu Basin, Jackson et al. (2018) suggested that the maximum depositional age of the Relu Basin strata is 45.5 ± 0.5 Ma, and the most likely age of the Relu Basin is early Oligocene. He et al. (2022) observed several pyroclastic rocks and volcanic tuffs in the lower middle part of the Relu Basin, which yielded U—Pb ages of 48–40 Ma. They also conducted a detrital zircon U—Pb study on the sandstones from the lowest part of the Relu Basin, which suggested a maximum deposition age of ~50 Ma. Based on these age constraints, together with the mammalian fossils *Yuomys* sp., discovered at the lower part of the Relu Basin that indicate a middle Eocene age (Ni et al., 2023), He et al. (2022) concluded that the Relu Basin sediments accumulated during 50–34 Ma (Fig. 5s).

In the Mangkang Basin, the Lawula Formation comprises andesitic agglomerates, trachytes, and andesites in the lower part, and purple-red and grey-yellow tuffaceous sandstones and siltstones in the upper part (Su et al., 2019). The Lawula Formation was assigned to the Late Miocene based on the presence of abundant spores and pollen (e.g., *Equisetum* sp., *Betula mankangensis*, *Carpinus* cf. *fargesiana*), plant macrofossils (*Pinus* sp., *P. yunnanensis*, *Cyperacites* sp.) (Tao and Du, 1987), ostracods (*Stenocypia fischeri*, *Candoniella donschanensis*), and gastropods (*Australorbis* cf. *peseudoammonius*) (BGMR Xizang, 1993). However, $^{40}Ar/^{39}Ar$ dating on volcanic rocks from the Lawula Basin suggested a late Eocene-early Oligocene age (36–33 Ma) for the upper part of the Lawula Formation (Su et al., 2019, Fig. 5l). Recently, Zhao et al. (2023) reported several U—Pb dating ages on the interbedded volcanic rocks within the Lawula Formation and constrained the Lawula Formation to between 42 Ma and 36 Ma, the slight age difference might be due to the methodology of radiometric dating used in each study. In general, the Lawula Formation is late Eocene-early Oligocene in age rather than Late Miocene.

3.2. Cenozoic stratigraphy in the Yunling collage

To the south of eastern Tibet lies the Yunling collage, which is surrounded by the Yulong thrust fault to the north, the Jinhe-Qinghe thrust fault and the Chenghai fault to the southeast, and the Diancang Shan shear zone to the southwest (Fig. 2). Cenozoic sediments in the Yunling collage are mainly deposited in the Jianchuan, Lijiang, Yongsheng, and Yanyuan basins (Fig. 2), and have been divided into the Paleocene Yunlong and Guolang formations, the Eocene Baoxiangsi Formation, the Oligocene Jinsichang Formation, the Miocene Shuanghe Formation, and the Pliocene Jianchuan and Sanying formations from old to young (YBGMR, 1990, Fig. 3). This area was previously thought to have accumulated the most continuous sedimentary succession on the SEMTP, especially in the Jianchuan Basin.

The Yunlong and Guolang formations are mainly deposited in the Jianchuan Basin (also called Mengyejing Formation in some case, e.g., Gourbet et al. (2017)). The Yunlong Formation mainly consists of red to violet, thin-bedded horizontally-laminated mudstones and marlstones, and contains gypsum (Fig. 4a); while the Guolang Formation is composed primarily of purple-red mudstones and siltstones interbedded with red sandstones. The Yunlong and Guolang formations were assigned to the Paleocene based on the presence of gastropods (e.g., *Assiminea retopercula*, *Bithynia yunlongensis*), ostracods (e.g., *Cyprinotus* cf. *lectus*, *Sinocypris* sp., *Limnocythere menglaensis*, *Limnocythere yunlongensis*), and some plant fossils (YBGMR, 1990). Gourbet et al. (2017) merged the Yunlong and Guolang formations together into the Mengyejing Formation (the earliest Cenozoic sediments in the Lanping-Simao fold belt, see Section 3.6), and assigned a Paleocene to early Eocene age to it. However, a recent magnetostratigraphic study in the Jiangcheng Basin (see Fig. 2 for location) suggested that the Mengyejing Formation is Late Cretaceous-early Paleocene in age (~112–63 Ma) (Yan et al., 2021). In addition, the *Re*—Os age of bitumen hosted in the breccia-bearing sandstones of the Yunlong Formation was determined to be 68 ± 5 Ma (Gao et al., 2012) or 59 ± 2 Ma (Sun et al., 2021), which further constrained the Yunlong Formation as Late Cretaceous-early Paleocene in age.

The Baoxiangsi Formation unconformably overlies the Guolang Formation and is mainly deposited in the Jianchuan and Yongsheng basins. It is dominated by massive breccias composed of exclusively angular to subangular, poorly sorted limestone clasts, interbedded with sandstones in the lower part, and massive red sandstones with an abundance of planar cross-bedding in the upper part (YBGMR, 1990, Fig. 4b). The Baoxiangsi Formation is well-known for the presence of

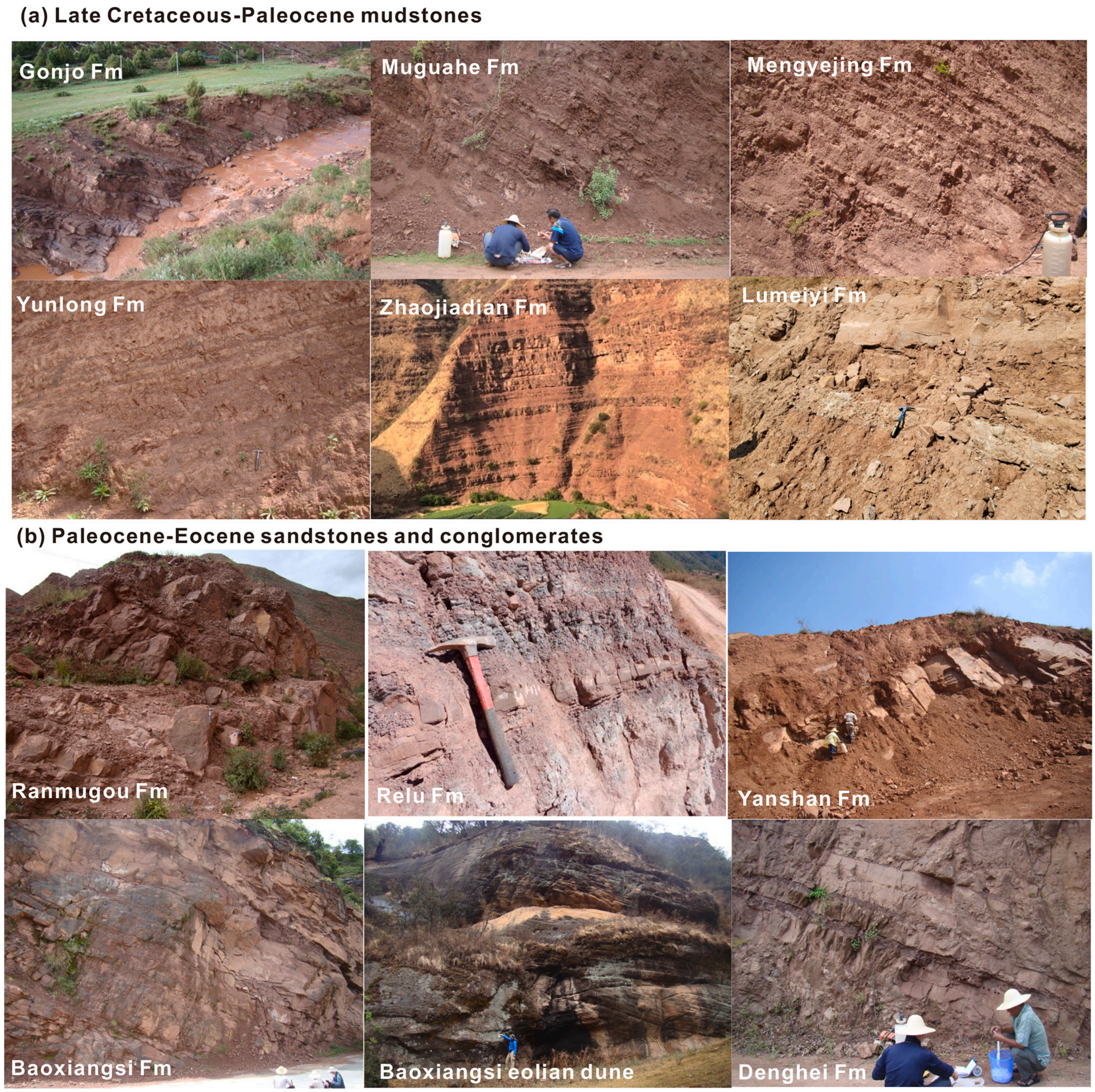

Fig. 4. Photos show (a) the Late Cretaceous-early Paleocene mudstones, and (b) the Paleocene-early Eocene sandstones, conglomerates, and eolian dune deposits in the southeast margin of the Tibetan Plateau.

eolian dune deposits in both Jianchuan and Yanyuan basins (Jiang et al., 2012; Zheng et al., 2022; Fig. 4b). Sporopollen, plant fossils and mammalian elements such as *Eoentelodon likiangensis*, *Lunania* cf. and *Honanodon hebertis* suggested an Eocene age for the Baoxiangsi Formation (YBGMR, 1990). A magnetostratigraphic study of the Baoxiangsi Formation in the Jianchuan Basin suggested an age of 50–40 Ma (Luo et al., 2020), which is consistent with the 41 Ma upper age of the Baoxiangsi Formation (Fig. 5m), also defined by magnetostratigraphy with U—Pb ages from tuff layer as anchor point by Fang et al. (2021). However, we note that the magnetostratigraphic study of Luo et al. (2020) did not reach the bottom of the Baoxiangsi Formation, thus the basal age of the Baoxiangsi Formation should be older than 50 Ma.

Above the Baoxiangsi Formation is the Jinsichang Formation in the Jianchuan Basin or the Lijiang Formation in Lijiang Basin, both of which are mainly comprise of clast-supported and/or matrix-supported conglomerates interbedded with coarse sandstones, fine-grained sandstones and siltstones (YBGMR, 1990; Wei et al., 2016, Fig. 6a). Only a few plant groups, such as *Myrica* cf. *angustifolia* and Taxodiaceae, have been recovered and described from the Jinsichang Formation, which was previously suggested as being of Oligocene age. There is no absolute age constraint on this formation due to the lack of suitable dating materials.

The Shuanghe Formation is made of thinly-laminated mudstones, siltstones and fine sandstones (Fig. 5b). This formation is well-known for the presence of coal beds and an abundance of plant groups comprising the “Shuanghe flora” upon which the original ‘Miocene’ age was based (Editorial Committee of Cenozoic Flora of China, 1978; YBGMR, 1990). The Jianchuan Formation consists of trachytes, volcanic breccias, and tuffs, interbedded with volcano-sedimentary and pyroclastic rocks (Fig. 5b), and was assigned to the Late Miocene-Early Pliocene based on stratigraphic correlation (YBGMR, 1990) and apatite fission track (AFT) ages (Xiang et al., 2009). However, recent zircon U—Pb and $^{40}Ar/^{39}Ar$ dating of interbedded and cross-cutting magmatic rocks within the

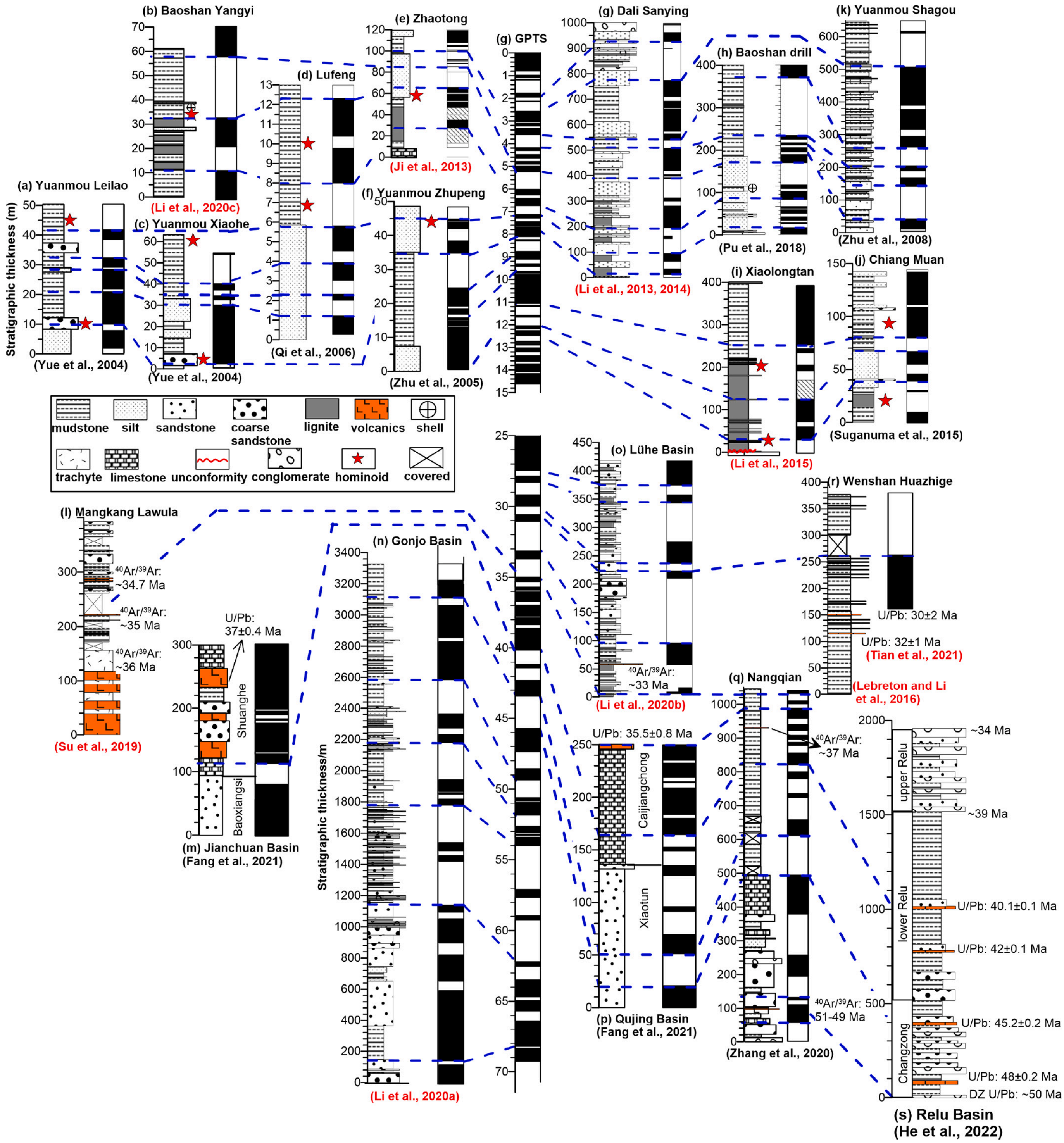

Fig. 5. The available new age constraints on the Cenozoic sediments in the southeast margin of the Tibetan Plateau.

Shuanghe and Jianchuan formations suggest a late Eocene age for both the Shuanghe and Jianchuan formations (Hoke et al., 2014; Yang et al., 2014; Gourbet et al., 2017; Zheng et al., 2021). Therefore, the Jinsichang Formation between Baoxiangsi and Shuanghe formations should be early late Eocene in age. Notably, Gourbet et al. (2017) discovered a ~ 100 m thick limestone succession at the bottom of the Shuanghe Formation which they defined as the Jiuziyan Formation that should also be late Eocene in age (Fig. 5b).

The Sanying Formation is only developed in the southeastern corner of the Jianchuan Basin and Yanyuan Basin in the Yunling collage (Fig. 2). It is mainly comprised of grey and yellow mudstones, interbedded with yellow sandstones and black-grayish lignites (Wang et al., 1998; Li et al., 2013, Figs. 7h and7i). The Sanying Formation contains abundant plant fossils, termed collectively the "Sanying flora", including those assigned to *Quercus pannosa (*H.-M.*)*, *Q. semecarpifolia*, *Q. gilliana*, *Acer paxii*, *Pinus yunnanensis*, and *Celtis bungeana* (Tao and Kong, 1973). In addition, Zong et al. (1996) described some mammal fossils, including *Sinomastodon yanyuanensis*, *Stegodon elephantoides*, *Chilotherium* sp., *Cervavitus* sp., and *Gomphotherium* sp.. Based on the evidence of these fossil records, a Late Pliocene age was originally suggested for the

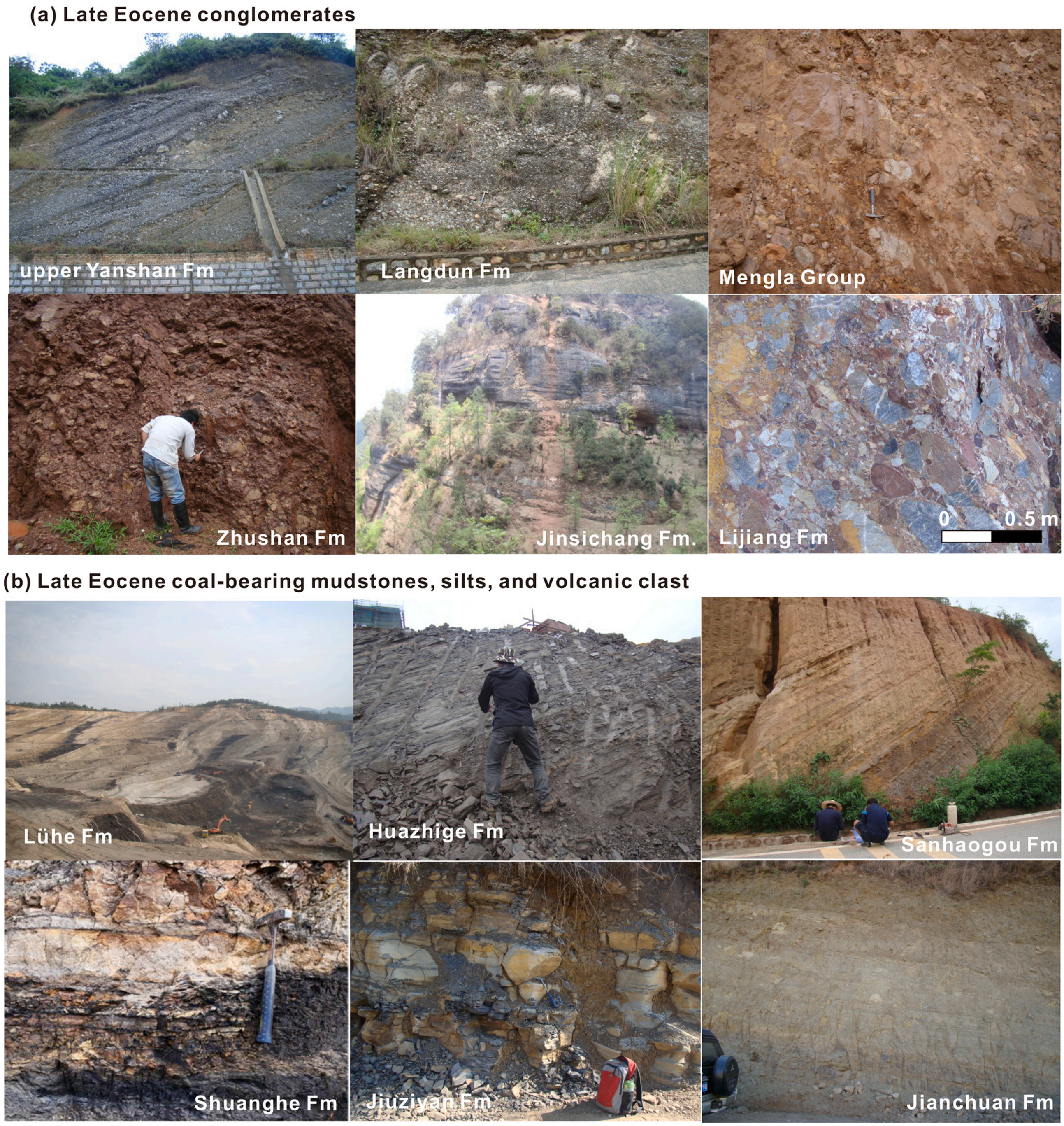

Fig. 6. Photos show (a) the early late Eocene conglomerates and (b) late Eocene coal-bearing sediments in the southeast margin of the Tibetan Plateau.

Sanying Formation (YBGMR, 1990). However, a magnetostratigraphic study suggests a Late Miocene-Pleistocene age (Li et al., 2013, Fig. 5g).

3.3. Cenozoic stratigraphy in the Chuxiong Basin

The Chuxiong Basin lies between the Chenghai fault to the west, the Yuanmou fault (one branch of the Xianshuihe-Xiaojiang fault) to the east, and the Ailao Shan shear zone to the southwest (Fig. 2). Cenozoic sediments are mainly deposited around the Yuanmou area, and are divided into the supposedly Paleocene Zhaojiadian Formation, the late Oligocene-Early Miocene Langdun Formation, Late Miocene Shihuiba or Xiaolongtan Formation, and the Pliocene Shagou Formation (YBGMR, 1990, Fig. 3).

The Zhaojiadian Formation is well developed around the Yuanmou area (Fig. 2), and consists of red-colored mudstones, siltstones, and fine sandstones (Fig. 4a). It conformably overlies the Jiangdihe Formation (YBGMR, 1990). Only limited plant fossils have been discovered from the Zhaojiadian Formation, but numerous Early Cretaceous-Paleocene charophytes, ostracods and a fish fauna have been reported from the underlying Jiangdihe Formation (YBGMR, 1990; Xing et al., 2018). Therefore, a Paleocene age is roughly attributed to the Zhaojiadian Formation.

The Langdun Formation is only developed at the front of the Ailao Shan shear zone (Fig. 2), and is dominated by limestone conglomerates and sandstones (Schoenbohm et al., 2005, Fig. 6a). Schoenbohm et al. (2005) identified a few plant macrofossils in the Langdun Formation and suggested a late Oligocene to Early Miocene age for this formation.

The Xiaolongtan Formation is supposedly of Late Miocene age and

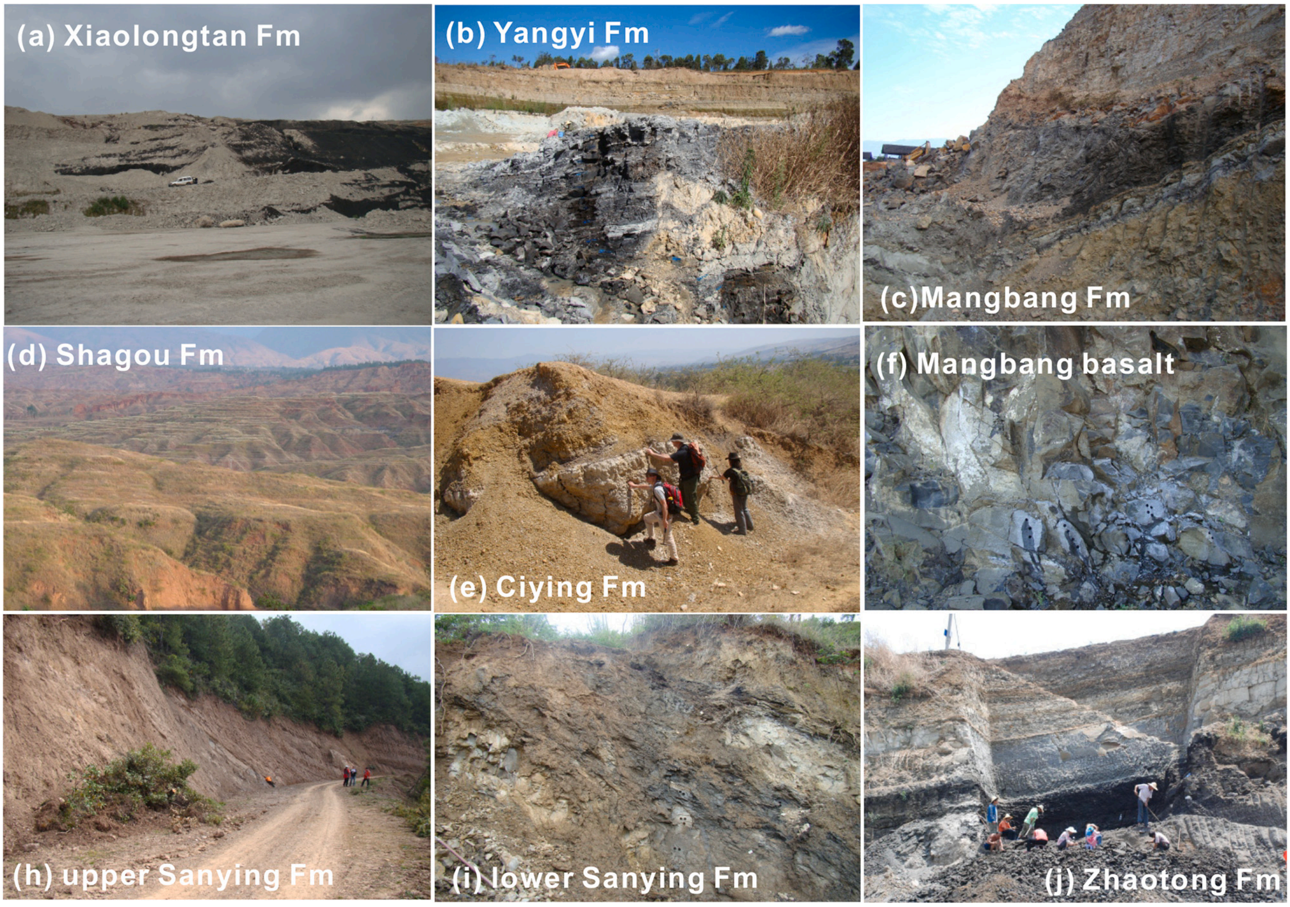

Fig. 7. Photos show the Neogene coal-bearing fine-grained sediments in the southeast margin of the Tibetan Plateau.

has been recognized in the Lühe Basin, while a Late Miocene age is also attributed to the Shihuiba Formation from the Yuanmou Basin (Fig. 3). The sediments in the Lühe Basin are dominated by marlstones, mudstones, sandstones, and lignites (Fig. 7b). Numerous leaf, fruit, and seed fossil groups and a palynoflora, comprising taxa such as *Tsuga* sp., *Calocedrus* sp., *Metasequoia* sp., *Carpinus* sp., *Alnus* sp., *Picea* sp., and *Quercus* sp., are preserved in the Lühe Basin (Xu et al., 2008). The flora assemblages are similar to elements found in other Late Miocene floras in Xiaolongtan and, therefore, a Late Miocene age was assigned to the Lühe Basin (YBGMR, 1990; Wang, 1996; Xu et al., 2008). However, magnetostratigraphy, anchored by zircon U—Pb and $^{40}Ar/^{39}Ar$ dating on interbedded tuffs, revised the age of Lühe Basin from Late Miocene to late Eocene-early Oligocene (35–26.5 Ma) (Linnemann et al., 2018; Li et al., 2020b, Fig. 5o). Subsequently, the age of sediments exposed in the lower part of the Lühe coal mine has been further refined using astronomically forced cyclostratigraphy (Xu et al., 2023). Since the age of the Lühe Basin is significantly older than the Xiaolongtan Formation in the Xiaolongtan Basin of the Yangtze Platform (see Section 3.4), we use Lühe Formation for the sediments in Lühe Basin to discriminate it from the Xiaolongtan Formation in Xiaolongtan Basin.

The Shihuiba Formation is mainly deposited in the Yuanmou and the adjacent Lufeng basins (Fig. 2), and is dominated by fine sandstones. It is well-known for yielding the hominoid fossil *Lufengpithecus lufengensis* (Woo et al., 1981). In addition, numerous mammalian fossils such as *Prodendrogale yunnanica, Ptilocercinae* gen. et sp. *indet.*, *Hylomys* aff. *Suillus*, and *Yunoscaptor scalprum* have also been recovered from the Yuanmou Basin (Qi et al., 2006). To constrain the age of the hominoid *Lufengpithecus lufengensis,* several magnetostratigraphic studies have been undertaken on the Yuanmou and Lufeng basins, which suggest a 11–7 Ma age of the Shihuiba Formation (Yue et al., 2004; Zhu et al., 2005; Qi et al., 2006, Fig. 5a, c, d, and f).

The Shagou Formation is only developed in the Yuanmou Basin. It unconformably overlies the Shihuiba Formation, and is composed of fine-grained sandstones, peaty clays, siltstones, and rare interbedded conglomerates (Zhu et al., 2008a, Fig. 7d). The discovery of a *Homo* fossil in the Shagou Formation has made the Yuanmou Basin a focus for understanding human evolution (Hu, 1973). A high-resolution magnetostratigraphic study of the Shagou Formation dated it precisely as 4.9–1.4 Ma (Zhu et al., 2008a, 2008b, Fig. 5k).

3.4. Cenozoic stratigraphy in the Yangzi Platform

The Yangzi Platform refers to the area of northeast Yunnan east of the Yuanmou fault (Fig. 2). Cenozoic sediments in the Yangzi Platform are mainly developed along the branches of the Xianshuihe-Xiaojiang fault and accumulated in the Kunming, Xianfeng, and Zhaotong basins. The Cenozoic succession is divided into the Lumeiyi, Xiaotun, Caijiangchong, Xiaolongtan, and Ciying formations from old to young (YBGMR, 1990, Fig. 3).

The Lumeiyi Formation is mainly deposited in the Kunming, Lunan, and Mile basins (Fig. 2). It is dominated by red-colored siltstones, sandstones and interbedded grey clay-limestones (YBGMR, 1990, Fig. 4a). Abundant mammalian fossils, e.g., *Lephialetes expeditus*, *Helaletes mongoliensis*, *Dianotitan lunanensis*, and *Cadurcodon ardynensisi* have been recovered from the Lumeiyi Formation, suggesting an Eocene age (YBGMR, 1990).

The Xiaotun and Caijiangchong formations are mainly developed in the Qujing Basin (Fig. 2). The Xiaotun Formation comprises mainly purple-brown red fine conglomerates, sandstones and mudstones that contain salts and gypsum, while the Caijiangchong Formation is dominated by grayish, greenish, or yellowish clays and clay-limestones (YBGMR, 1990; Fang et al., 2021). The Xiaotun and Caijiangchong formations were previously assigned an Oligocene age due to the preservation of mammalian fossils such as *Cadurcodon ardynensisi*, *Gigantamynodom gigianteus*, and *Bothriodon chowi* et. (YBGMR, 1990). However, Fang et al. (2021) observed a 5-m thick tuff layer at the top of the Caijiangchong Formation in the Qujing Basin, which gave a U—Pb age of ~36 Ma. This, together with magnetostratigraphy, constrains the Xiaotun Formation to span 47–41 Ma, and Caijiangchong Formation 41–36 Ma (Fig. 5p).

The Xiaolongtan Formation is mainly developed in Xiaolongtan and Xianfeng basins, and consists of coal-bearing mudstones, clay-limestones, and siltstones (Fig. 7a). As well as the noted hominoid fossil *Lufengpithecus keiyuanensis*, numerous vertebrate fossils (e.g., *Tetralophodon xiaolohgtanensis*, *Gomphotherum* cf. *macrognathus*, *Zygolophodon chinjiensis*, *Tapirus* cf. *yunnanensis*, and *Euprox* sp.) and plant fossils (e.g., Fabaceae, Fagaceae, and Lauraceae) are also preserved in the Xiaolongtan Formation (Editorial Committee of Cenozoic Flora of China, 1978; Zhou, 1985; Dong, 1987; Zhang, 1987; Wang, 1996; Pickford and Liu, 2001; Dong and Qi, 2013), which indicate a Middle-Late Miocene age for the Xiaolongtan Formation. The magnetostratigraphy of the Xiaolongtan Basin suggests an age of ~14–10 Ma (Li et al., 2015; Zhang et al., 2019, Fig. 5j), consistent with the biostratigraphic age framework.

The Ciying Formation is preserved in many pull-apart basins along the Xianshuihe-Xiaojiang fault, e.g., Kunming, Qujing, and Jianshui basins (Fig. 2). The Ciying Formation mainly comprises multi-colored mudstones, siltstones, and sandstones (Fig. 7e). Besides the earliest peach fossil, *Prunus kunmingensis*, reported from this formation (Su et al., 2015), mammalian fossils, such as *Stegodon yuanmouensis*, *S. Zhaotonggensis*, *S. elephantoides*, and *Stogolophodon banguoensis* indicate a Pliocene age for the Ciying Formation (YBGMR, 1990), which is consistent with the 4.8–1.7 Ma age indicated by a magnetostratigraphic study from the Jianshui Basin (Xiong et al., 2016). In the Zhaotong Basin, the Zhaotong Formation is dominated by lignites and dark grey silty clays (Fig. 7j). The Zhaotong Basin is also well-known for the preservation of the hominoid fossil *Lufengpithecus lufengensis* (Ji et al., 2013). In addition, typical Late Miocene mammalian fossils *Stegodon zhaotongensis* and *Sinomastodon* sp. and rich plant fossils such as *Carya*, *Corylus*, *Euryale* and *Trapa* were also observed from the Zhaotong Basin (Ji et al., 2013; Huang et al., 2017a). Magnetostratigraphy, together with these biostratigraphic constraints, constrains the Zhaotong Formation to span 7.3–2.6 Ma (Ji et al., 2013, Fig. 5e).

3.5. Cenozoic stratigraphy in the South China fold and thrust belt

The South China fold and thrust belt is the area of southeast Yunnan east of the Mile fault (Fig. 2). Cenozoic sediments only contain Yanshan and Huazhige formations around the Wenshan area (Fig. 3). The Yanshan Formation is dominated by grey-, yellow-, and light red-colored conglomerates interbedded with red sandstones (YBGMR, 1990, Fig. 4b). Only a limited number of fossils have been discovered from the Yanshan Formation, and a preliminary Eocene age was assigned to the Yanshan Formation based on stratigraphic correlation (YBGMR, 1990). The Huazhige Formation unconformably overlies the Yanshan Formation and consists of grey and dark-grey mudstones and siltstones (Fig. 6b). Numerous plant fossils, e.g., *Rosa fortuita*, *Exbucklandia acutifolia*, have been reported from this formation (Su et al., 2016; Huang et al., 2017b). It was previously inferred to be deposited at the same time as the Xiaolongtan Formation, during the Middle-Late Miocene, based on the similarity of some plant fossils found from both formations (YBGMR, 1990). Lebreton-Anberrée et al. (2016) tried to constrain the age of the Huazhige Formation by magnetostratigraphy, but only obtained two magnetozones due to the shortness of the available section, and they tentatively suggested a late Early Miocene age. However, Tian et al. (2021) observed two layers of volcanic ashes in the upper part of the Huazhige Formation, which yielded U—Pb ages of ~30 Ma and ~32 Ma, separately, suggesting an early Oligocene age (Fig. 5r).

3.6. Cenozoic stratigraphy in the Lanping-Simao fold belt

The Lanping-Simao fold belt is sandwiched by the Ailao Shan-Red River shear zone to the east, and the Chongshan shear zone-Changning granite belt to the west (Fig. 2). Cenozoic sediments in the Lanping-Simao fold belt are mainly deposited in the Lanping, Jinggu, and Mengla basins, and are grouped into the Mengyejing Formation, the Denghei Formation, the Mengla Group, the Sanhaogou Formation, and the Sanying Formation from old to young (YBGMR, 1990, Fig. 3). Notably, the Cenozoic sediments in the Lanping-Simao fold belt have very similar lithologies to those of the Jianchuan Basin (see Section 3.2). The Mengyejing Formation mainly consists of evaporite-bearing (halite and gypsum) red mudstones, siltstones, and interbedded fine sandstones (YBGMR, 1990; Yan et al., 2021, Fig. 4a). The age of the Mengyejing Formation is vital due to the bearing of potash mines, but is highly controversial, ranging from Jurassic to Paleocene (see Yan et al., 2021). Based on a high-resolution magnetostratigraphic study of the Mengyejing Formation in the Jiangcheng area (see Fig. 2 for location), together with detrital zircon U—Pb ages from the sandstones, Yan et al. (2021) constrained the age of the Mengyejing Formation be from ~112–63 Ma.

The Denghei Formation conformably overlies the Mengyejing Formation. It is dominated by alternating layers of red fine-grained siltstones and mudstones (Fig. 4b). The age of the Denghei Formation is considered to be Eocene based on regional stratigraphic correlations, and its fossil content of ostracods (*Paraleptestheria menglaensis*, *Sinocypris* sp.), charophytas (*Harrisichara yunlongensis*, *Peckichara varians*, and *Stephanochara breviovalis*), and gastropods (*Assiminea retopercula*, *Bithynia yunlongensis*) (YBGMR, 1990). The Mengla Group unconformably overlies the Denghei Formation and is dominated by matrix-supported conglomerates, and massive coarse-grained sandstones interbedded with thin mudstones (Fig. 6a). Only very few plant fossils have been discovered from the Mengla Group, and an Oligocene age has been suggested based on regional stratigraphic correlations in the traditional geological map (YBGMR, 1990). No updated age constraints exist for the Denghei Formation and Mengla Group.

The Sanhaogou Formation unconformably overlies the Mengla Group and mainly outcrops around the Jinggu county (Fig. 2). It consists of red-grayish to black mudstones, grey and yellow sandstones, several (sandy) conglomerates, and lignites (Fig. 6b). Besides some ostracods, gastropods, and fish fossils, abundant plant fossils have been found in the Sanhaogou Formation, which collectively form the "Jinggu flora" (Editorial Committee of Cenozoic Flora of China, 1978; YBGMR, 1990). Based on floristic comparison with neighboring areas, a Middle Miocene age was estimated for the Sanhaogou Formation in the geological map of Yunnan Province (YBGMR, 1990).

The Sanying Formation is only occasionally developed in the Lanping-Simao fold belt, e.g., Zhenyuan and Jingdong (Fig. 2), and has the same lithology as the Sanying Formation in the Jianchuan and Dali basins, and therefore should also be Late Miocene-Pleistocene as in the Yunling collage (Li et al., 2013).

3.7. Cenozoic stratigraphy in the Baoshan and Tengchong terranes

The Basoshan and Tengchong terranes lie in western Yunnan and are separated from each other by the Gaoligong shear zone (Fig. 2). Cenozoic sediments in the Baoshan terrane are mainly assigned to the Paleogene Muguahe and Zhushan formations in the Yongde Basin (YBGMR, 1990, Fig. 3). Neogene sediments called the Yangyi Formation (in some places also referred to as the Yingpan Formation) are only developed in a few small basins, such as the Baoshan and Gengma basins (YBGMR, 1990, Fig. 2). In the Tengchong terrane, only the Neogene Nanlin and Mangbang formations are developed in small basins among the Mesozoic-early Cenozoic intrusions and along the Gaoligong shear zone (Fig. 2).

The Muguahe Formation consists of brick red or purple-red mudstones and siltstones (YBGMR, 1990, Fig. 4a). It was assigned a Paleocene age based on the preservation of ostracods (*Cypridea speciosa* and *Porpocypris sphaeroidalis*) (YBGMR, 1990). The Zhushan Formation unconformably overlies the Muguahe Formation and is mainly composed of clast- or matrix-supported grey and purple-red conglomerates that are dominated by limestone clasts (Fig. 6a). No fossils have been recovered from the Zhushan Formation, and an Oligocene age has been suggested based on regional stratigraphic correlations (YBGMR, 1990).

The Yangyi Formation consists of black lignites interbedded with grey, yellow, and black mudstones and siltstones in the lower part, and grey, black, and maroon mudstones in the upper part (YBGMR, 1990; Li et al., 2020c, Fig. 7b). The Yangyi Formation preserves the youngest hominoid fossil *Lufengpithecus* sp. in the SEMTP (Harrison et al., 2002; Li et al., 2020c). Besides this, a number of other mammal fossils (e.g., *Stegodon baoshanensis*, *Stegolophodon yangyiensis*, and *Stegodon elephantoides*), shells of freshwater gastropods (*Cipangopaludina* sp., *Kwangsispira* sp., and *Semisulcospira* sp.), and plant fossils (including *Quercus pannosa*, and *Q. presenescens*) have been discovered in the Yangyi Formation of the Baoshan Basin (Jiang et al., 1983; Li et al., 2009). Moreover, a hominoid fossil was recovered from the Yangyi Formation in the Baoshan Basin (Xu, 1992). Based on these biostratigraphic constraints, magnetostratigraphic studies from the Baoshan Basin refined the Yangyi Formation as being from ~8–3 Ma (Pu et al., 2018; Li et al., 2020c, Fig. 5h). Notably, Sun et al. (2022) reported a magnetostratigraphic study on the Gengma Basin and suggested an Early Miocene age (~18–16 Ma) for the sediments in the Gengma Basin. However, since no isotopic age or fossils provide a clear age constraint anchor, the reliability of the correlation between the observed magnetozones to the global geomagnetic polarity time scales by Sun et al. (2022) remains uncertain. We therefore keep the Yangyi Formation as Late Miocene-Pliocene in age until such constraints become available.

In the Tengchong terrane, the Mangbang Formation unconformably overlies the Nanlin Formation (YBGMR, 1990, Fig. 2). The Nanlin Formation is dominated by grey and purple red conglomerates and coarse sandstones in the lower part, and grey and brown sandstones in the upper part. Some plant fossils including *Calocedrus lantenoisi*, *Dryophyllum yunnanense*, *Quercus parachampionii*, *Celtis bungeana*, and *Rhus* sp. have been observed in the Nanlin Formation, which was assigned to the Miocene for this formation in the traditional geological map (YBGMR, 1990). The Mangbang Formation is mainly composed of grey sandy conglomerates and sandstones at the bottom, several layers of basalts in the middle, and grey fine sandstones, mudstones, diatomites, and lignites at the top (Fig. 5c and f). Many fossils have been discovered at the top of the formation such as *Betula elliptica*, *Carpinus mangbangensis*, *Alnus longellipticus*, *Castanopsis predelavayi*, *Fagus chinensis*, *Quercus francentioides*, *Populus* sp., *Sorbus hemsleyi*, and *Acer pliocenicum*, which suggests a Pliocene age for the Mangbang Formation (Ge and Li, 1999). Moreover, K—Ar dating of the basalts interbedded in the Mangbang Formation and the andesitic rocks overlying the Mangbang Formation range from 7.2 Ma to 0.007 Ma (Li et al., 2000; Wang et al., 2008a), which constrains the Mangbang Formation at Late Miocene-Pliocene.

4. Updated age framework for the Cenozoic stratigraphy in the southeast margin of the Tibetan Plateau

Based on the new age constraints on many sedimentary basins as described in Section 3, we build an updated age framework for the Cenozoic stratigraphy in the SEMTP (Fig. 8).

The earliest Cenozoic sediments in the SEMTP are best constrained for the Mengyejing Formation in the Yunling collage and Lanping-Simao belt (Yan et al., 2021), and the Gonjo Formation and lower Ranmugou Formation in the Gonjo Basin (Li et al., 2020a), which were deposited during the Late Cretaceous-early Paleocene rather than just the Paleocene as traditionally estimated. Typically, the sediments deposited at this time are characterized by gypsum-bearing red-colored mudstones, siltstones, and interbedded fine sandstones (Fig. 4a). Similar sediments include those of the Zhaojiadian Formation in the Chuxiong Basin and the Muguahe Formation in the Baoshan terrane, and perhaps part of the Lumeiyi Formation in the Yangzi Platform (Figs. 4a and 9), all of which seem to be Late Cretaceous-early Paleocene in age.

Above the Late Cretaceous-early Paleocene sediments are Paleocene-early Eocene units, including the middle and upper Ranmugou Formation in the Gonjo Basin (55.5–41.5 Ma, Li et al., 2020a), the Ranmugou Formation in the Nangqian Basin (52–35 Ma, Zhang et al., 2020), the Changzong and lower Relu Formation in the Relu Basin (~50–39 Ma, He et al., 2022), the Baoxiangsi Formation in the Jianchuan Basin (>50–40 Ma, Luo et al., 2020; Fang et al., 2021; Zheng et al., 2021), and the Xiaotun Formation in the Qujing Basin (47–41 Ma, Fang et al., 2021). The sediments deposited during this interval are typically made by red interbedded conglomerates and sandstones (Figs. 4b and 9). Moreover, eolian dune deposits are developed in several basins, such as the Jianchuan, Yongsheng, and Relu basins (Jiang et al., 2012; He et al., 2022; Zheng et al., 2022) (Fig. 4b). Similar sediments, also deposited in Paleocene-early Eocene, occur in part of the Lumeiyi, Yanshan and Denghei formations (Figs. 4b and 9).

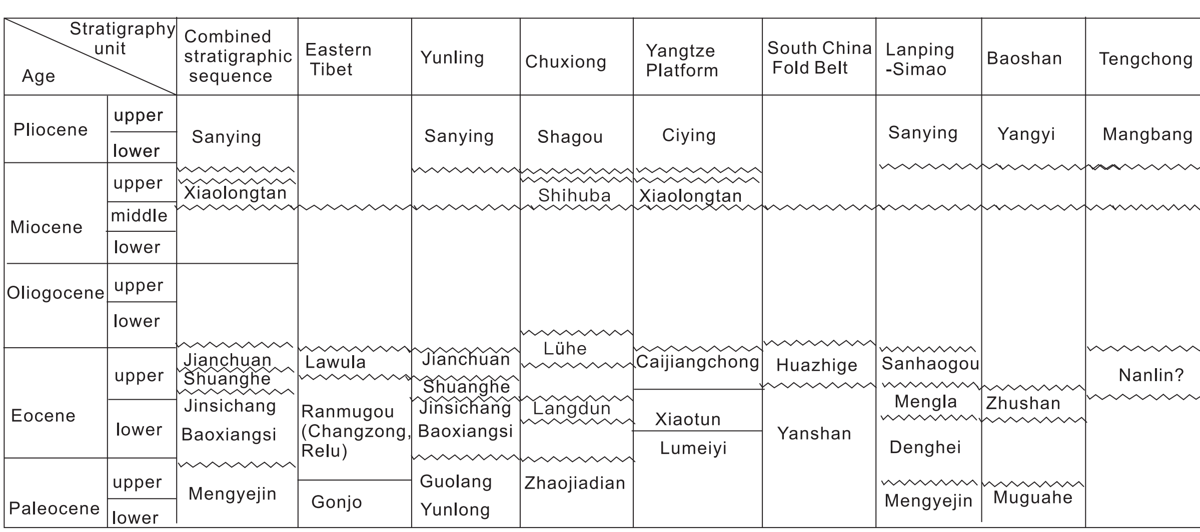

Fig. 8. The updated Cenozoic stratigraphy framework in the southeast margin of the Tibetan Plateau based on new age constraints from Fig. 5.

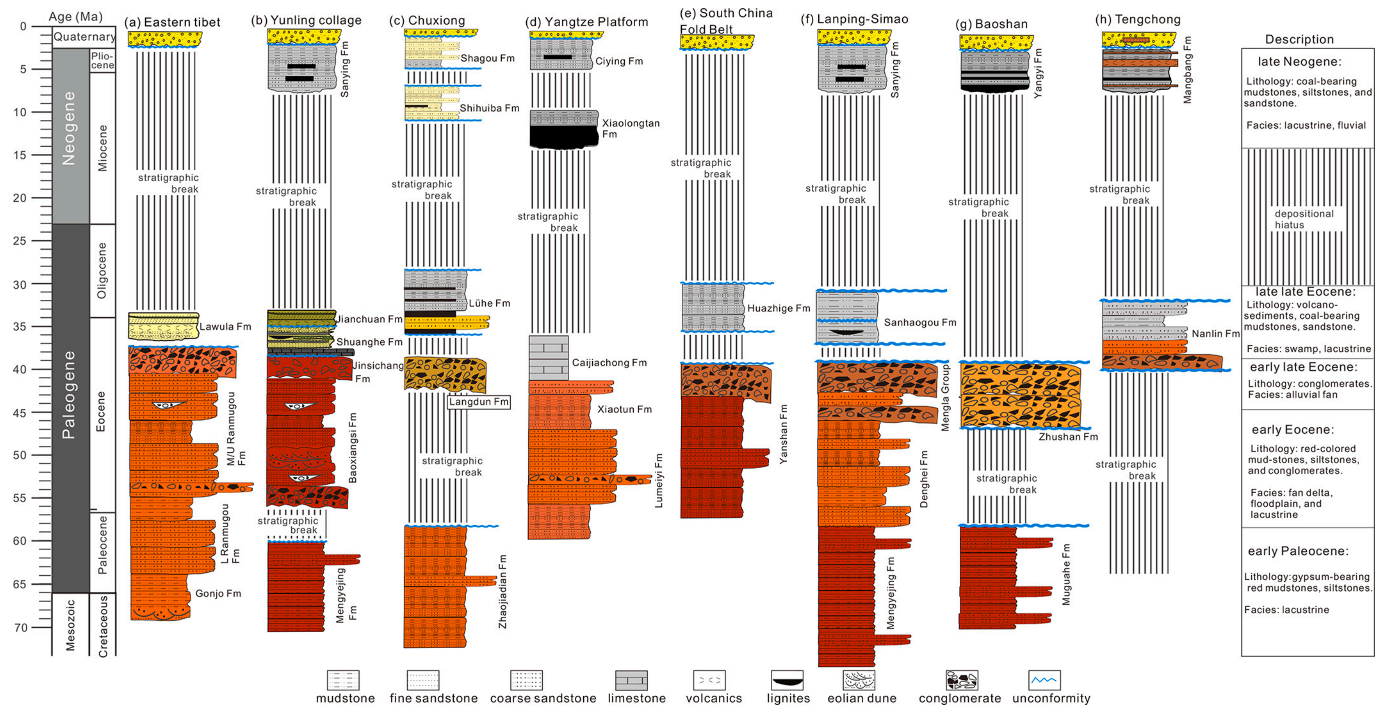

Fig. 9. Correlation of the Cenozoic stratigraphy from different stratigraphic units in the southeast margin of the Tibetan Plateau based on the updated age framework.

Above the Paleocene-early Eocene sediments, early late Eocene deposits are dominated by typical limestone conglomerates (Figs. 6a and 9), which are widespread across the whole area. For example, they occur in the upper Relu Formation in the Relu Basin (39–34 Ma, He et al., 2022), the Jinsichang Formation in the Jianchuan Basin, the Lijiang Formation in the Lijiang Basin, the Mengla Group in the Jinggu Basin, the Langdun Formation in the Yuanjiang Basin, and the Zhushan Formation in the Yongde Basin (Fig. 6a). The Jinsichang Formation is indirectly constrained between ~40–37 Ma by the underlying Baoxiangsi Formation (~50–40 Ma) and the overlying Shuanghe and Jianchuan formations (~37–34 Ma, Gourbet et al., 2017; Luo et al., 2020; Fang et al., 2021). Apart from the well-dated upper Relu and Jinsichang formations, no reliable age constraints are available for the other formations in the SEMTP, but we consider that all these conglomerates dominated by limestone clasts were deposited contemporaneously in the late Eocene (Figs. 8 and 9).

The latest Paleogene sediments in the SEMTP are represented by the Shuanghe and Jianchuan formations (Fig. 8), which consist of coal-bearing grey and dark grey mudstones, siltstones and fine sandstones, and volcano-sedimentary and pyroclastic rocks (Figs. 6b and 9). Similar sediments are found in the Lawula Formation in the Mangkang Basin (>42–33 Ma, Su et al., 2019; Zhao et al., 2023), the Lühe Formation in the Lühe Basin (~35–26.5 Ma; Li et al., 2020b), the Caijiangchong Formation in the Qujing Basin (41–36 Ma, Fang et al., 2021), and the Huazhige Formation in the Wenshan Basin (>30 Ma, Lebreton-Anberrée et al., 2016; Tian et al., 2021). We tentatively consider that the Sanhaogou Formation in the Jinggu Basin and the Nanlin Formation in the Tengchong terrane were also deposited in the latest Eocene due to the similar lithologies, but future studies are needed to assess the validity of this hypothesis (Figs. 8 and 9).

Early Neogene sediments are only developed in the Chuxiong Basin (the Shihuiba Formation) and the Yangtze Platform (the Xiaolongtan Formation) (Fig. 8), which have been well dated to span ~11–7 Ma (Yue et al., 2004; Zhu et al., 2005; Qi et al., 2006) and ~ 14–10 Ma (Li et al., 2015; Zhang et al., 2019), respectively. These sediments are dominated by lignites, grey mudstones and siltstones (Figs. 7a and 9). Late Neogene sediments are characterized by coal-bearing fine grained mudstones, siltstones, and sandstones with rare conglomerates (Figs. 7b-7j). They are widespread in many sedimentary basins mainly along strike-slip faults in the SEMTP (Fig. 2), e.g., the Sanying Formation in the Jianchuan and Dali basins (7.6–1.8 Ma, Li et al., 2013), the Shagou Formation in the Yuanmou Basin (4.9–1.4 Ma, Zhu et al., 2008a), the Ciying Formation in the Jianshui Basin (4.8–1.7 Ma, Xiong et al., 2016), the Zhaotong Formation in the Zhaotong Basin (7.3–2.6 Ma, Ji et al., 2013), the Yangyi Formation in the Baoshan Basin (~8–3 Ma, Pu et al., 2018; Li et al., 2020c), and the Mangbang Formation in the Tengchong Basin (~7–0 Ma, Li et al., 2000; Wang et al., 2008a, Fig. 9).

With these new age constraints, we find that the most significant change for the updated age framework for Cenozoic sediments in the SEMTP is that many sediments that were previously assigned to "Oligocene-Late Miocene" based on biostratigraphic age and regional stratigraphic correlations are now revised to be late Eocene to early Oligocene (Fig. 8, such as the upper Lawula Formation in the Mangkang Basin (Su et al., 2019), the Jianchuan and Shuanghe formations in the Jianchuan Basin (Gourbet et al., 2017), the Lühe Formation in the Lühe Basin (Linnemann et al., 2018; Li et al., 2020b), and the Huazhige Formation in the Wenshan Basin (Tian et al., 2021). The updated age framework suggests that the Cenozoic sediments in the SEMTP were not deposited continuously, but instead displays a paucity of late Oligocene-Middle Miocene sediments (Figs. 8 and 9).

Our updated age framework for the Cenozoic stratigraphy in the SEMTP is based on a large number of new age data by different methods, such as magnetostratigraphy, isotopic dating on interbedded volcanic rocks, and mammal fossils (Fig. 5), which provide by far the most complete and reliable age constraints on the Cenozoic sediments in the SEMTP. However, we realize that reliable dating on the Paleogene stratigraphy is still limited, and some of the correlations of stratigraphy between different units are mainly based on similar lithologies, e.g., the Muguahe Formation from the Baoshan terrane to the Mengyejing Formation from the Lanping-Simao fold belt. Therefore, more studies focusing on the age of Paleogene basins in the SEMTP are essential to confirm such correlations in the future.

5. Discussion

5.1. Depositional environments and structures of the Cenozoic sedimentary basins in the southeast margin of the Tibetan Plateau

As described in Section 4, within the updated age framework for the Cenozoic stratigraphy in the SEMTP, the Late Cretaceous-early Paleocene sediments are characterized by gypsum-bearing red-colored mudstones, siltstones, and interbedded fine sandstones (Fig. 4a), suggesting lacustrine facies with variable lake extent and episodic arid playa lake conditions (Fig. 9). The overlying Paleocene-early Eocene sediments are made of red-colored interbedded conglomerates, sandstones, and

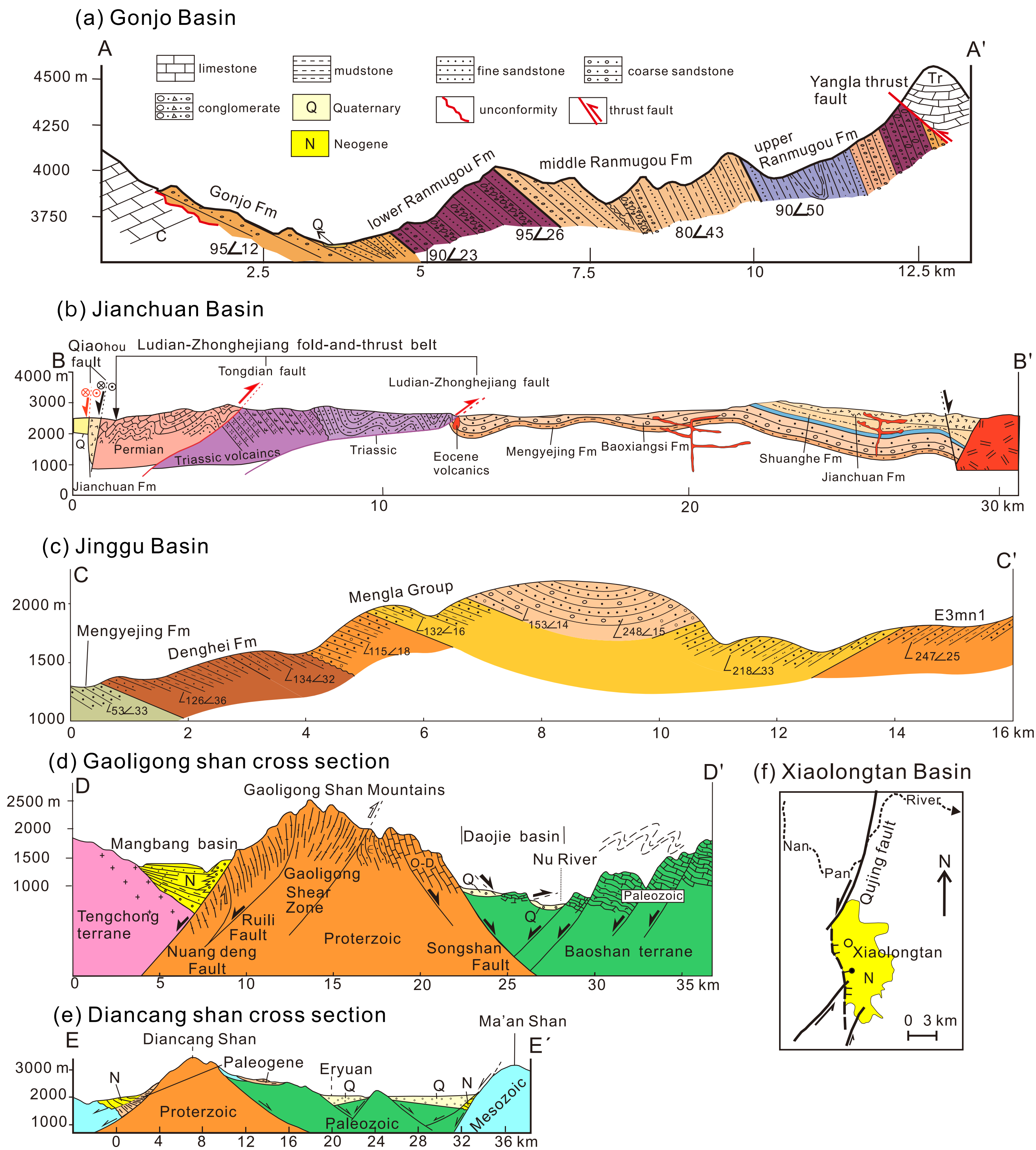

Fig. 10. Typical sedimentary basin structures in the southeast margin of the Tibetan Plateau. The cross-section of (a) Gonjo Basin, (b) Jianchuan Basin, and (c) Jinggu Basin is modified from Li et al. (2020a), Cao et al. (2020), and Li et al. (2017b), respectively. The cross-section of the (d) Gaoligong Shan and (e) Diancang Shan is modified from Wang et al. (2008a) and Li et al. (2014), respectively. (f) The morphology of the pull-apart Xiaolongtan Basin, cited from Wang et al. (1998) and Li et al. (2015). See Fig. 2 for the locations of the cross-sections.

mudstones (Fig. 4b), indicating fan-delta, floodplain and lacustrine depositional environments (Fig. 9). The presence of eolian dune deposits during this interval indicates a dry and hot climatic background. The early late Eocene sediments are dominated by red and purple-red conglomerates (Fig. 6a), indicating alluvial fan and fluvial fan facies. The latest Eocene-early Oligocene sediments are composed of volcano-sedimentary rocks and coal-bearing grey, dark grey mudstones, siltstones and fine sandstones (Fig. 6b), suggesting swamp and lacustrine facies. The change from red-colored sandstones and conglomerates to coal-bearing grey mudstones marks an important change from a dry and hot climate to a humid condition in the late Eocene (Fig. 9), which evidences a marked increase of rainfall which some interpret as the initiation or enhancement of a monsoon system (Sorrel et al., 2017; Fang et al., 2021; Zheng et al., 2022), although the exact transition time and monsoon characteristics are still being explored (He et al., 2022).

The Neogene sediments are also dominated by lignites and dark grey mudstones in their lower parts, and multi-colored mudstones, siltstones, and sandstones in the upper parts (Fig. 7). Based on detailed magnetostratigraphic studies, we consider that the last lignite formation ended at ~6 Ma in several basins, e.g. the Zhaotong, Dali, and Baoshan basins (Ji et al., 2013; Li et al., 2013; Li et al., 2020c), which coincides with the extinction of hominoids in the SEMTP (Ji et al., 2013; Li et al., 2020c). The change from lignites to mudstones, siltstones, and sandstones at ~6 Ma suggests a further aridification from a mildly warm and humid climate in swamp environments to lacustrine and fluvial environments (Zhang et al., 2016a; Li et al., 2020d), which may have contributed to the disappearance of hominoids from this region (Li et al., 2020c). Multiple explanations have been suggested for this transition, such as rapid uplift of the Tibetan Plateau (e.g., Clark et al., 2005), the enhancement of the East Asia monsoon (An et al., 2001), and/or the global cooling (Zachos et al., 2008), but in light of recent advances in understanding landscape, climate and biotic evolution in the region, these causes are unlikely, but a detailed discussion is beyond the scope of this study.

In addition to the depositional environments, we also examined the sedimentary structures of several basins in the SEMTP, which show strong differences between the Paleogene and Neogene.

Generally, Paleogene basins were deposited in compressional settings and experienced strong folding and deformation. For example, in the Gonjo Basin, the Yangla thrust fault carried Triassic rocks over the basin margin in the northeast, forming an asymmetric syncline (Fig. 10a). The strata in the western limb are significantly thicker and shallower than those in the eastern limb (Studnicki-Gizbert et al., 2008; Li et al., 2020a, Fig. 10a), and growth strata were developed in the basin. In addition, anisotropy of magnetic susceptibility studies from the Gonjo Basin recorded an enduring NE-SW shortening during its deposition (Li et al., 2020e; Xiao et al., 2021; Tong et al., 2022). These lines of evidence suggest that the Gonjo Basin was a syntectonic basin in a contractional setting. Similar sedimentary structures were also observed in the Lühe Basin (Li et al., 2020b). In the Jianchuan Basin, the Ludian-Zhonghejiang fault carried the Triassic rocks over the Cenozoic sediments and growth strata were formed at the bottom of the Baoxiangsi Formation (Cao et al., 2020, Fig. 10b). Low-temperature thermochronology from Triassic plutons in the hanging wall of the Ludian-Zhonghejiang fault indicates a rapid exhumation during 50–39 Ma (Cao et al., 2020), which is synchronous with the deposition age of the Baoxiangsi and Jinsichang formations. This means that the Paleogene Jianchuan Basin was also a syntectonic basin in a contractional setting. In the Lanping-Simao fold belt and the Chuxiong Basin, the Paleogene and Mesozoic sediments experienced strong folding (e.g., the Jinggu Basin (Fig. 10c), Burchfiel and Chen, 2012; Li et al., 2017b,), and were unconformably overlain by weakly deformed Neogene sediments with shallow dips (e.g., Wang et al., 1998).

In contrast to the compressional settings for Paleogene sedimentary basins, Neogene basins were mostly deposited in extensional settings. In the cross-sections of the Gaoligong Shan and Diancang Shan, the Neogene basins in both sides of the Gaoligong Shan and Diancang Shan were formed as graben or half-graben (Fig. 10d and e). The sediments in these basins (e.g., the Mangbang, Dali, and Eryuan basins) dip to the normal fault (Fig. 10d and e), indicating that these basins were filled during activity of the normal faults in front of the mountains (e.g., Wang et al., 2008a). Moreover, many Neogene basins, especially those along the branches of the Xianshuihe-Xiaojiang fault, were developed as pull-apart (e.g., the Xiaolongtan Basin, Fig. 10f) or sag basins to accommodate the left slip on the Xianshuihe-Xiaojiang fault (Wang et al., 1998).

5.2. *Tectonic implications on the uplift of the southeast margin of the Tibetan Plateau*

The updated age framework for the Cenozoic stratigraphy in the SEMTP shows that:

1) Early Paleocene sediments are mainly lacustrine fine-grained deposits without deformation structures, suggesting that these sediments were deposited in a relative quiet tectonic period (Fig. 11a).

2) Eocene sediments unconformably overlie the early Paleocene sediments, and mainly consist of alluvial fan sandstones, and conglomerates, especially in the early late Eocene. The conglomerates are poorly sorted, and are dominated by limestones, sandstone, and volcanics (Fig. 6a), which apparently were derived from proximal older rocks (Horton et al., 2002; Spurlin et al., 2005; Studnicki-Gizbert et al., 2008; Cao et al., 2020; Li et al., 2024), implying marked relief, with variable

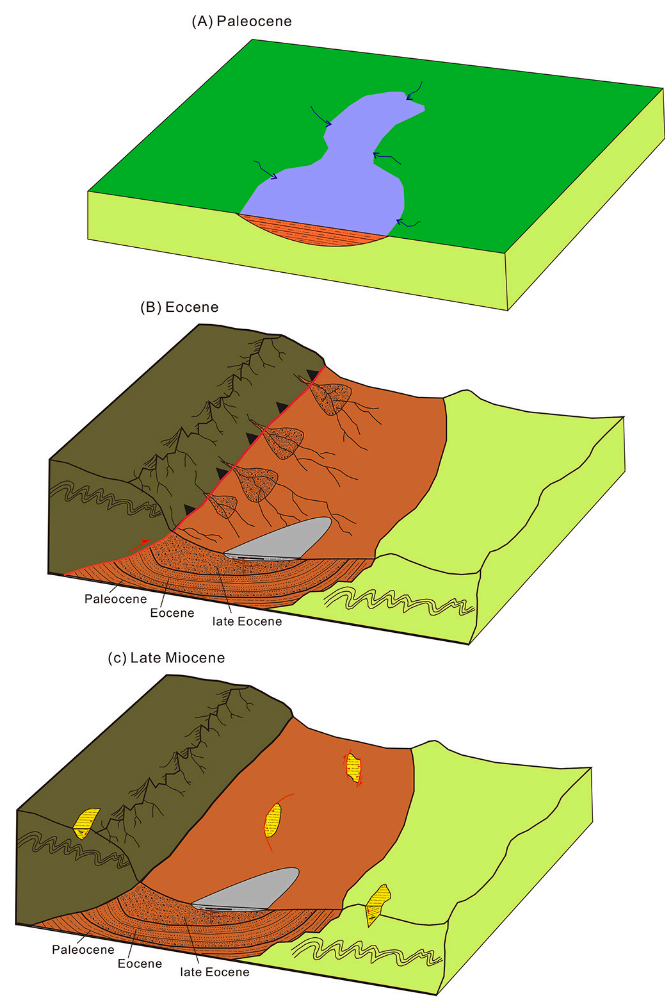

Fig. 11. Craton illustrating the tectonic deformation and sediments deposition at (a) Paleocene, (b) Eocene, and (c) Late Miocene in the southeast margin of the Tibetan Plateau. Modified from Cao et al. (2020).

quantities of episodic runoff from mountain slopes. Moreover, the Eocene sediments are syntectonic accumulations in contractional settings. All these lines of evidence suggest that the SEMTP experienced significant crustal shortening and uplift beginning in the early Eocene (~50 Ma) (Fig. 11b), shortly after the hard continental collision of India with Eurasia (e.g., Li et al., 2020a; Yuan et al., 2021).

3) Paleogene sediments generally ended in the early Oligocene, while Neogene sedimentation began at scale after the Middle Miocene. It seems that there was a significant depositional hiatus between Oligocene and Middle Miocene, which probably suggests that the SEMTP had attained most of its current elevation by the end of the late Eocene, and then under relatively weak erosion few sediments were deposited between the Oligocene and Middle Miocene. There are probably some local exceptions, such as in the case of the early Oligocene Lühe Basin, but the overall pattern is clear. The long-term erosion between the Oligocene and Middle Miocene may have facilitated the formation of the low-relief southeast margin of the Tibetan Plateau, supporting the idea that the relict landscape was most likely formed at high elevation (Liu-Zeng et al., 2008) instead of at sea level (Clark et al., 2006).

4) Neogene sediments are generally weakly deformed and deposited in extensional settings (Fig. 11c), which further indicates that no significant shortening and uplift occurred in the SEMTP after the Middle Miocene.

Our results suggest that the SEMTP underwent rapid deformation and uplift beginning in the late early Eocene, and may have achieved its near current elevation by the end of the Eocene. This conclusion is supported by numerous previous studies. First, large amounts of low temperature thermochronological data suggested that the SEMTP underwent a rapid exhumation during the Eocene (Zhang et al., 2016b; Liu-Zeng et al., 2018; Cao et al., 2020; Tao et al., 2022; Tian et al., 2022; Zhang et al., 2022) and early Oligocene (Tian et al., 2014; Wang et al., 2012; Shen et al., 2016; Wang et al., 2022a, Fig. 12), which was related to crustal shortening and regional denudation as revealed by our reviews of the sedimentary records. Second, a series of paleoaltimetry studies have suggested that the SEMTP rose rapidly after ~50 Ma, and had almost attained its current elevation by the end of the Eocene (Hoke et al., 2014; Gourbet et al., 2017; Tang et al., 2017; Wu et al., 2018; Su et al., 2019; Xiong et al., 2020; He et al., 2022; Zhao et al., 2023, Fig. 12). For example, paleoelevation studies from the Jianchuan Basin suggested that it underwent a rapid uplift in the early Eocene (Gourbet et al., 2017; Wu et al., 2018), although they applied different methods and concluded different paleoelevations for the Jianchuan Basin. In the Mangkang Basin, paleoelevation estimates using plant fossils suggested that the basin rose quickly from ~3 km in the late Eocene (~34 Ma) to its present elevation (3.9 km) in the latest Eocene-earliest Oligocene (Su et al., 2019; Zhao et al., 2023). Paleoelevation studies using stable isotope suggested that the Gonjo Basin rose from ~0.7 km in the early Eocene to ~3.8 km in the middle Eocene (Xiong et al., 2020), while the Relu Basin uplifted from 0.6 ± 0.6 km at ~50–45 Ma to 2.0 ± 0.9 km at 45–42 Ma, to 2.9 ± 0.9 km at 42–40 Ma, and finally attained its modern elevation (3.5 ± 1.0 km) at 39–34 Ma (He et al., 2022). The early Cenozoic deformation in the SEMTP is also documented by structural shortening (Fig. 12), such as folding and thrusting in and around the Red River fault (e.g., Zhang et al., 2017; Liang et al., 2022) and Chuxiong fault (Li et al., 2020b), early Cenozoic duplexing in the Longmen Shan (Tian et al., 2016), increased sedimentation rates and shortening strain of the Gonjo (Li et al., 2020a, 2020e) and Nangqian basins (Zhang et al., 2020), vertical axis rotations (Li et al., 2017a; Li et al., 2020a; Zhang et al., 2020), and possible drainage network reorganization caused by surface uplift (e.g., Zheng et al., 2021).

Notably, a large number of low-temperature thermochronological data suggested rapid river incision or exhumation starting at ~15–10 Ma in the SEMTP (e.g., Clark et al., 2005; Ouimet et al., 2010; Wang et al., 2012; Tian et al., 2015; Zhang et al., 2016b; Pitard et al., 2021; Replumaz et al., 2020; Shen et al., 2022, Fig. 12), which was considered as evidence of rapid surface uplift at that time due to lower crustal flow (e.g., Clark et al., 2005), or rock uplift over a crustal ramp (Tian et al., 2013, 2016; Shen et al., 2019, 2022). The extensional settings of the Neogene sedimentary basins in the SEMTP, however, do not support significant uplift of the region after the Middle Miocene. Some moderate uplift of mountains, e.g., Gaoligong Shan and Ailao Shan, may have been due to isostatic rebound of river incision, but rapid river incision in the Miocene could have been the result of an enhanced monsoon (Nie et al., 2018), base-level fall caused by fault-related river captures (Hoke et al.,

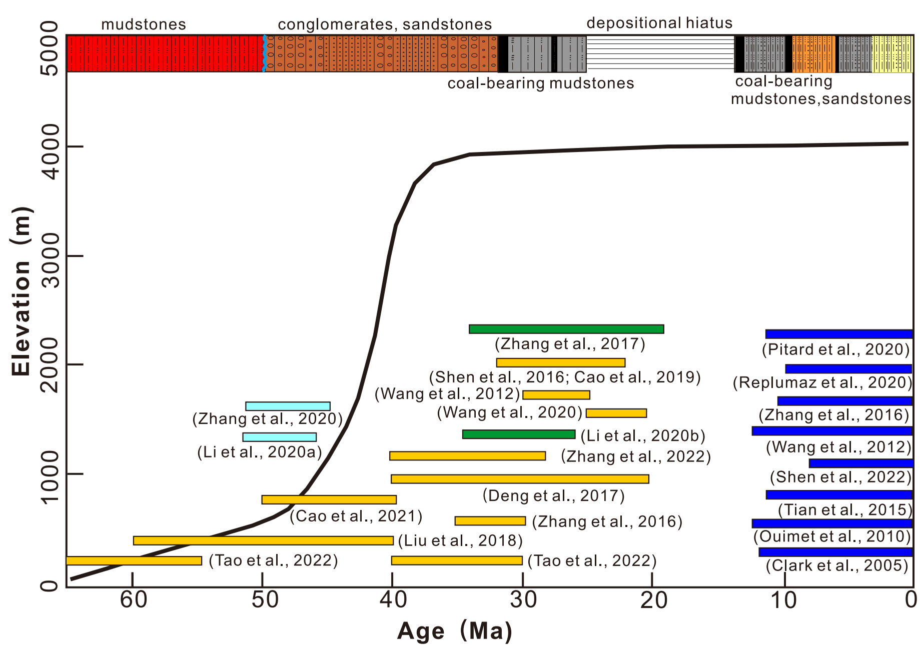

Fig. 12. Carton showing the correlations among sedimentation, paleoelelation (black line, modified from Zhao et al. (2023)), and tectonic deformations of the southeast margin of the Tibetan Plateau. The yellow and blue bars denote rapid exhumation of the southeast margin of the Tibetan Plateau in early Cenozoic and Late Miocene, respectively, as suggested by low-temperature thermochronological data. The bars in green and light blue represent fault activity with shortening and vertical axis rotation, respectively. (For interpretation of the references to colour in this figure legend, the reader is referred to the web version of this article.)

2014), headward drainage basin expansion (Rohrmann et al., 2023), or a combination thereof.

6. Concluding remarks

In this study we have reviewed recent improvements regarding the dating of Cenozoic sediments in the southeast margin of the Tibetan Plateau (SEMTP), and built an updated age framework for the Cenozoic stratigraphy for this area. Our revised age framework transforms the traditional view that the Cenozoic sediments were deposited continuously in the SEMTP, but instead show Oligocene-Middle Miocene sediments are largely absent. Moreover, many sedimentary basins in the SEMTP that were previously assigned an "Oligocene-Late Miocene" age based largely on well-preserved plant fossils and inter-basin correlations were actually formed in the Eocene. The updated age framework, together with depositional environment and sedimentary structure analysis of basins, suggests that the SEMTP underwent rapid deformation and uplift beginning in the early Eocene, and achieved its near-present elevation at the end of the Eocene. This is consistent with regional quantitative paleoelevation evidence. By the Middle Miocene, extensional tectonics dominated the region and further uplift was minimal, being confined to isostatic adjustment following erosion.

CRediT authorship contribution statement

Shihu Li: Conceptualization, Data curation, Formal analysis, Funding acquisition, Investigation, Methodology, Project administration, Resources, Writing – original draft, Writing – review & editing. **Robert A. Spicer:** Funding acquisition, Investigation, Writing – original draft, Writing – review & editing, Data curation. **Tao Su:** Data curation, Funding acquisition, Investigation, Writing – original draft, Writing – review & editing. **Zhekun Zhou:** Data curation, Funding acquisition, Investigation, Writing – original draft, Writing – review & editing. **Chenglong Deng:** Conceptualization, Data curation, Funding acquisition, Investigation, Supervision, Writing – original draft, Writing – review & editing.

Declaration of competing interest

The authors declare that they have no known competing financial interests or personal relationships that could have appeared to influence the work reported in this paper.

Data availability

No data was used for the research described in the article.

Acknowledgements

We would like to thank Prof. Xiumian Hu and Prof. Shitao Zhang for helpful discussions, and Dr. Weiyu Wang and Zhiming Fu for help in figure preparation. The manuscript was significantly improved by invaluable comments from editor Jimin Sun and two anonymous reviewers. This research was funded by the National Natural Science Foundation of China (NSFC, No. 41888101), National Key Research and Development Program of China (No. 2023YFF0804503), and NSFC (No. 92155203). This work was also partly funded by NSFC–NERC joint research program nos. 42320104005 and NE/P013805/1.

References

An, Z., Kutzbach, J.E., Prell, W.L., Porter, S.C., 2001. Evolution of Asian monsoons and phased uplift of the Himalayan Tibetan plateau since late Miocene times. Nature 411, 62–66.
Bertrand, G., Rangin, C., 2003. Tectonics of the western margin of the Shan plateau (Central Myanmar): implication for the India – Indochina oblique convergence since the Oligocene. J. Asian Earth Sci. 21, 1139–1157.
Bertrand, G., Rangin, C., Maluski, H., Bellon, H., 2001. Diachronous cooling along the Mogok Metamorphic Belt (Shan scarp, Myanmar): the trace of the northward migration of the Indian syntaxis. J. Asian Earth Sci. 19, 649–659.
BGMR Sichuan, 1991. Regional Geology of Sichuan Province. Geological Memoirs Series. Geological Publishing House, Beijing, pp. 1–730.
BGMR Xizang, 1993. Regional Geology of Xizang (Tibet) Autonomous Region. Geological Memoirs Series. Geological Publishing House, Beijing, pp. 1–707.
Burchfiel, B.C., Chen, Z., 2012. Tectonics of the southeastern Tibetan Plateau and its adjacent foreland. Geol. Soc. Am. Memoirs 210, 1–165.
Cao, K., Leloup, P.H., Wang, G., Liu, W., Mahéo, G., Shen, T., Xu, Y., Sorrel, P., Zhang, K., 2020. Thrusting, exhumation, and basin fill on the western margin of the South China block during the India-Asia collision. Geol. Soc. Am. Bull. 133, 74–90.
Chung, S.L., Lee, T.Y., Lo, C.H., Wang, P.L., Chen, C.Y., Yem, N.T., Hoa, T.T., Wu, G.Y., 1997. Intraplate extension prior to continental extrusion along the Ailao Shan Red River shear zone. Geology 25, 311–314.
Clark, M., Schoenbohm, L.M., Royden, L.H., Whipple, K.X., Burchfiel, B.C., Zhang, X., Tang, W., Wang, E., Chen, L., 2004. Surface uplift, tectonics, and erosion of eastern Tibet from large-scale drainage patterns. Tectonics 23, TC1006.
Clark, M., House, M.A., Royden, L.H., Whipple, K.X., Burchfiel, B.C., Zhang, X., Tang, W., 2005. Late Cenozoic uplift of southeastern Tibet. Geology 33, 525–528.
Clark, M., Royden, L., Whipple, K., Burchfiel, B., Zhang, X., Tang, W., 2006. Use of a regional, relict landscape to measure vertical deformation of the eastern Tibetan Plateau. J. Geophys. Res. 111, F03002.
Curray, J.R., 2005. Tectonics and history of the Andaman Sea region. J. Asian Earth Sci. 25, 187–232.
Ding, W.N., Ree, R.H., Spicer, R.A., Xing, Y.W., 2020. Ancient orogenic and monsoon-'riven assembly of the world's richest temperate alpine flora. Science 369, 578–581.
Dong, W., 1987. Further investigations upon the age and characteristics of the Xiaolongtan fauna, Kaiyuan Co. Yunnan Province. Vert. Palas. 25, 116–123.
Dong, W., Qi, G., 2013. Hominoid-producing localities and biostratigraphy in Yunnan. In: Wang, X.M., Flynn, L.J., Fortelius, M. (Eds.), Fossil Mammals of Asia—Neogene Bio-Stratigraphy and Chronology. Colombia University Press, New York, pp. 293–313.
Editorial Committee of Cenozoic Flora of China, 1978. Plant fossils of China. In: Cenozoic Flora of China, vol. 3. Science Press, Beijing.
England, P., Molnar, P., 1990. Right-lateral shear and rotation as the explanation for strike-slip faulting in eastern Tibet. Nature 344, 140–142.
Fang, X., Yan, M., Zhang, W., Nie, J., Han, W., Wu, F., Song, C., Zhang, T., Zan, J., Yang, Y., 2021. Paleogeography control of Indian monsoon intensification and expansion at 41 Ma. Sci. Bull. 66, 2320–2328.
Favre, A., Packert, M., Pauls, S.U., Jahnig, S.C., Uhl, D., Michalak, I., Muellner-Riehl, A. N., 2015. The role of the uplift of the Qinghai-Tibetan Plateau for the evolution of Tibetan biotas. Biol. Rev. 90, 236–253.
Fyhn, M., Boldreel, L.O., Nielsen, L.H., 2009. Geological development of the Central and south Vietnamese margin: Implications for the establishment of the South China Sea, Indochinese escape tectonics and Cenozoic volcanism. Tectonophysics 478, 184–214.
Gao, B., Xue, C.J., Chi, G.X., Li, C., Qu, W.J., Du, A.D., Li, Z.X., Gu, H., 2012. Re-Os dating of bitumen in the giant Jinding Zn-Pb deposit, Yunnan and its geological significance. Acta Petrol. Sin. 28, 1561–1567.
Ge, H., Li, D., 1999. Cenozoic Coal-Bearing Basins and Coal-Forming Regularity in West Yunnan. Yunnan Science and Technology Press, Kunming, pp. 1–132.
Gourbet, L., Leloup, P.H., Paquette, J.L., Sorrel, P., Maheo, G., Wang, G., Xu, Y., Cao, K., Antoine, P.-O., Eymard, I., Liu, W., Lu, H., Replumaz, A., Chevalier, M.L., Zhang, K., Jing, W., Shen, T., 2017. Reappraisal of the Jianchuan Cenozoic basin stratigraphy and its implications on the SE Tibetan plateau evolution. Tectonophysics 700–701, 162–179.
Guo, S.X., 1986. An Eocene Flora from the Relu Formation in Litang County and the History of *Eucalyptus,* Exploration of Hengduan Mountain Area, vol. 2. Beijing Publishing House of Sciences and Technology, Beijing, pp. 66–70.
Harrison, T., Ji, X.P., Su, D., 2002. On the systematic status of the late Neogene hominoids from Yunnan Province, China. J. Hum. Evol. 43, 207–227.
He, S., Ding, L., Xiong, Z., Spicer, R.A., Farnsworth, A., Valdes, P.J., Wang, C., Cai, F., Wang, H., Sun, Y., Zeng, D., Xie, J., Yue, Y., Zhao, C., Song, P., Wu, C., 2022. A distinctive Eocene Asian monsoon and modern biodiversity resulted from the rise of eastern Tibet. Sci. Bull. 67, 2245–2258.
Hoke, G.D., 2018. Geochronology transforms our view of how Tibet's southeast margin evolved. Geology 46, 95–96.
Hoke, G.D., Liu-Zeng, J., Hren, M.T., Wissink, G.K., Garzione, C.N., 2014. Stable isotopes reveal high southeast Tibetan Plateau margin since the Paleogene. Earth Planet. Sci. Lett. 394, 270–278.
Horton, B.K., Yin, A., Spurlin, M.S., Zhou, J.Y., Wang, J.H., 2002. Paleocene-Eocene syncontractional sedimentation in narrow, lacustrine-dominated basins of east-Central Tibet. Geol. Soc. Am. Bull. 114, 771–786.
Hu, C., 1973. Ape-man teeth from Yuanmou, Yunnan. Acta Geol. Sin. 1, 65–72.
Huang, J., Shi, G.L., Su, T., Zhou, Z.K., 2017b. Miocene *Exbucklandia (Hamamelidaceae)* from Yunnan, China and its biogeographic and palaeoecologic implications. Rev. Palaeobot. Palynol. 244, 96–106.
Huang, Y.J., Ji, X.P., Su, T., Deng, C.L., Ferguson, D.K., Yu, T.S., Yang, X., Sun, H., Zhou, Z.K., 2017a. Habitat, climate and potential plant food resources for the late Miocene Shuitangba hominoid in Southwest China: insights from carpological remains. Palaeogeogr. Palaeoclimatol. Palaeoecol. 470, 63–71.
Jackson, W.T., Robinson, D.M., Weislogel, A.L., Jian, X., McKay, M.P., 2018. Cenozoic development of the nonmarine Mula basin in the southern Yidun terrane: deposition and deformation in the eastern Tibetan Plateau associated with the India-Asia collision. Tectonics 37, 2446–2465.

Ji, X., Jablonski, N.G., Su, D.F., Deng, C.L., Flynn, L.J., You, Y., Kelley, J., 2013. Juvenile hominoid cranium from the terminal Miocene of Yunnan, China. Chin. Sci. Bull. 58, 3771–3779.
Jiang, N., Xiao, Y.F., Yang, Z.C., 1983. The discovery of the *Stegolophodon* from Yangyi of Baoshan County, Yunnan. Contribution to the Geology of the Qinghai-Xizang (Tibet). Plateau 11, 255–258.
Jiang, X.S.J., Cui, X., Wu, H., Xiong, G., Zhuo, J., Lu, J., Jiang, Z., 2012. The Paleogene deserts and their implications for the origin of monsoons on the eastern margin of the Qinghai-Xizang Plateau, SW China. Sediment. Geol. Tethyan Geol. 32 (3), 54–63.
Lacassin, R., Replumaz, A., Leloup, P.H., 1998. Hairpin river loops and slip-sense inversion on southeast Asian strike-slip faults. Geology 26, 703–706.
Lebreton-Anberrée, J., Li, S., Li, S.-F., Spicer, R.A., Zhang, S.-T., Su, T., Deng, C., Zhou, Z.-K., 2016. Lake geochemistry reveals marked environmental change in Southwest China during the Mid Miocene Climatic Optimum. Sci. Bull. 61, 897–910.
Leloup, P., Lacassin, R., Tapponnier, P., Scharer, U., Zhong, D.L., Liu, X.H., Zhang, L.S., Ji, S.C., Trinh, P.T., 1995. The Ailao Shan-Red River shear zone (Yunnan, China), Tertiary transform boundary of Indochina. Tectonophysics 251, 3–84.
Li, D., Li, Qi, Chen, W.J., 2000. Volcanic activities in the Tengchong volcano area since Pliocene. Acta Petrol. Sin. 16 (3), 362–370.
Li, N., Sun, B.N., Wu, J.Y., Yan, D.F., Xiao, L., Dai, J., 2009. Cuticular structure of *Quercus presenescens* from the Pliocene in Baoshan, Yunnan, and its paleoclimatic implications. Acta Paleontol. Sin. 48, 654–661.
Li, P., Zhang, C., Kelley, J., Deng, C., Ji, X., Jablonski, N.G., Wu, H., Fu, Y., Guo, Z., Zhu, R., 2020d. Late Miocene climate Cooling Contributed to the Disappearance of Hominoids in Yunnan Region, Southwestern China. Geophys. Res. Lett. 47, e2020GL087741.
Li, S., Deng, C.L., Yao, H.T., Huang, S., Liu, C.Y., He, H.Y., Pan, Y.X., Zhu, R.X., 2013. Magnetostratigraphy of the Dali Basin in Yunnan and implications for late Neogene rotation of the southeast margin of the Tibetan Plateau. J. Geophys. Res. 118, 791–807.
Li, S., Deng, C.L., Greig, P., Yao, H.T., Huang, S., Liu, C.Y., He, H.Y., Pan, Y.X., Zhu, R.X., 2014. Tectonic and sedimentary evolution of the late Miocene–Pleistocene Dali Basin in the southeast margin of the Tibetan Plateau: evidences from anisotropy of magnetic susceptibility and rock magnetic data. Tectonophysics 629, 362–377.
Li, S., Deng, C.L., Dong, W., Sun, L., Liu, S.Z., Qin, H.F., Yin, J.Y., Ji, X.P., Zhu, R.X., 2015. Magnetostratigraphy of the Xiaolongtan Formation bearing *Lufengpithecus keiyuanensis* in Yunnan, southwestern China: constraint on the initiation time of the southern segment of the Xianshuihe-Xiaojiang fault. Tectonophysics 655, 213–226.
Li, S., Advokaat, E.L., van Hinsbergen, D.J.J., Koymans, M., Deng, C., Zhu, R., 2017a. Paleomagnetic constraints on the Mesozoic-Cenozoic paleolatitudinal and rotational history of Indochina and South China: review and updated kinematic reconstruction. Earth Sci. Rev. 171, 58–77.
Li, S., Yang, Z., Deng, C., He, H., Qin, H., Sun, L., Yuan, J., van Hinsbergen, D.J.J., Krijgsman, W., Dekkers, M.J., Pan, Y., Zhu, R., 2017b. Clockwise rotations recorded in redbeds from the Jinggu Basin of northwestern Indochina. Geol. Soc. Am. Bull. 129, 1100–1122.
Li, S., Yin, C., Guilmette, C., Ding, L., Zhang, J., 2019. Birth and demise of the Bangong-Nujiang Tethyan Ocean: a review from the Gerze area of Central Tibet. Earth Sci. Rev. 198, 102907.
Li, S., van Hinsbergen, D.J.J., Najman, Y., Liu-Zeng, J., Deng, C., Zhu, R., 2020a. Does pulsed Tibetan deformation correlate with Indian plate motion changes? Earth Planet. Sci. Lett. 536, 116144.
Li, S., Su, T., Spicer, R.A., Xu, C., Sherlock, S., Halton, A., Hoke, G., Tian, Y., Zhang, S., Zhou, Z., Deng, C., Zhu, R., 2020b. Oligocene deformation of the Chuandian terrane in the SE margin of the Tibetan Plateau related to the extrusion of Indochina. Tectonics 39, e2019TC005974.
Li, S., Ji, X., Harrison, T., Deng, C., Wang, S., Wang, L., Zhu, R., 2020c. Uplift of the Hengduan Mountains on the southeastern margin of the Tibetan Plateau in the late Miocene and its paleoenvironmental impact on hominoid diversity. Palaeogeogr. Palaeoclimatol. Palaeoecol. 553, 109794.
Li, S., Hinsbergen, D.J.J., Shen, Z., Najman, Y., Deng, C., Zhu, R., 2020e. Anisotropy of magnetic susceptibility (AMS) analysis of the Gonjo Basin as an independent constraint to date Tibetan shortening pulses. Geophys. Res. Lett. 47, e2020GL087531.
Li, S., Najman, Y., Vermeesch, P., Barfod, D., Millar, I., Carter, A., 2024. A critical appraisal of the sensitivity of detrital zircon U–Pb provenance data to constrain drainage network evolution in southeast Tibet. J. Geophys. Res. 129, e2023JF007347 https://doi.org/10.1029/2023JF007347.
Li, S.F., Valdes, P.J., Farnsworth, A., Davies-Barnard, T., Su, T., Lunt, D.J., Spicer, R.A., Liu, J., Deng, W.Y., Huang, J., Tang, H., Ridgwell, A., Chen, L.L., Zhou, Z.K., 2021. Orographic evolution of northern Tibet shaped vegetation and plant diversity in eastern Asia. Sci. Adv. 7, eabc7741.
Liang, M., Yang, T., Xue, C., Xin, D., Yan, Z., Liao, C., Han, X., Xie, Z., Xiang, K., 2022. Complete deformation history of the transition zone between oblique and orthogonal collision belts of the SE Tibetan Plateau: crustal shortening and rotation caused by the indentation of India into Eurasia. J. Struct. Geol. 156, 104545.
Linnemann, U., Su, T., Kunzmann, L., Spicer, R.A., Ding, W.N., Spicer, T.E.V., Zieger, J., Hofmann, M., Moraweck, K., Gärtner, A., Gerdes, A., Marko, L., Zhang, S.T., Li, S.F., Tang, H., Huang, J., Mulch, A., Mosbrugger, V., Zhou, Z.K., 2018. New U–Pb dates show a Paleogene origin for the modern Asian biodiversity hot spots. Geology 46, 3–6.
Liu-Zeng, J., Tapponnier, P., Gaudemer, Y., Ding, L., 2008. Quantifying landscape differences across the Tibetan plateau: implications for topographic relief evolution. J. Geophys. Res. 113, F04018.
Liu-Zeng, J., Zhang, J., McPhillips, D., Reiners, P., Wang, W., Pik, R., Zeng, L., Hoke, G., Xie, K., Xiao, P., Zheng, D., Ge, Y., 2018. Multiple episodes of fast exhumation since cretaceous in Southeast Tibet, revealed by low-temperature thermochronology. Earth Planet. Sci. Lett. 490, 62–76.
Luo, C., Wang, P., Li, Y., Li, S., Wei, X., Huang, Y., 2020. Magnetostratigraphy of the Eocene Jianchuan Basin in southeast Tibet: A Preliminary Result. EGU General Assembly Conference Abstracts, p. 13422.
Mazur, S., Green, C., Stewart, M.G., Whittaker, J.M., Williams, S., Bouatmani, R., 2012. Displacement along the Red River Fault constrained by extension estimates and plate reconstructions. Tectonics 31, TC5008.
Metcalfe, I., 1996. Gondwanaland dispersion, Asian accretion and evolution of eastern Tethys. Aust. J. Earth Sci. 43, 605–623.
Mitchell, A., 1993. Cretaceous-Cenozoic tectonic events in the western Myanmar (Burma)-Assam region. J. Geol. Soc. Lond. 150, 1089–1102.
Mitchell, A., Chung, S.L., Oo, T., Lin, T.H., Hung, C.H., 2012. Zircon U–Pb ages in Myanmar: magmatic-metamorphic events and the closure of a neo-Tethys ocean? J. Asian Earth Sci. 56, 1–23.
Molnar, P., England, P., Martinod, J., 1993. Mantle dynamics, uplift of the Tibetan Plateau, and the Indian Monsoon. Rev. Geophys. 31, 357–396.
Morley, C.K., Arboit, F., 2019. Dating the onset of motion on the Sagaing fault: evidence from detrital zircon and titanite U–Pb geochronology from the North Minwun Basin, Myanmar. Geology 46, 581–585.
Ni, X., Li, Q., Deng, T., Zhang, L., Gong, H., Qin, C., Shi, J., Shi, F., Fu, S., 2023. New *Yuomys* rodents from southeastern Qinghai-Tibet Plateau indicate low elevation during the Middle Eocene. Front. Earth Sci. 10, 1018675.
Nie, J.S., Ruetenik, G., Gallagher, K., Hoke, G., Garzione, C.N., Wang, W.T., Stockli, D., Hu, X.F., Wang, Z., Wang, Y., Stevens, T., Danisik, M., Liu, S.P., 2018. Rapid incision of the Mekong River in the middle Miocene linked to monsoonal precipitation. Nat. Geosci. 11, 944–949.
Ouimet, W., Whipple, K., Royden, L., Reiners, P., Hodges, K., Pringle, M., 2010. Regional incision of the eastern margin of the Tibetan Plateau. Lithosphere 2, 50–63.
Pellegrino, A.G., Zhang, B., Speranza, F., Maniscalco, R., Yin, C., Hernandez-Moreno, C., Winkler, A., 2018. Tectonics and paleomagnetic rotation pattern of Yunnan (24°N-25°N, China): Gaoligong fault shear versus megablock drift. Tectonics 37, 1524–1551.
Pickford, M., Liu, L.P., 2001. Revision of the Miocene Suidae of Xiaolongtan (Kaiyuan), China. Boll. Soc. Paleontol. Ital. 40, 275–284.
Pitard, P., Replumaz, A., Chevalier, M.L., Leloup, P.H., Bai, M., Doin, M.P., Thieulot, C., Ou, X., Balvay, M., Li, H., 2021. Exhumation history along the Muli thrust—implication for crustal thickening mechanism in Eastern Tibet. Geophys. Res. Lett. 48 (14), e2021GL093677.
Pu, Z.W., Yang, Z.Y., Tong, Y.B., Zhao, Y., Wang, H., 2018. Paleomagnetic study of Pliocene lacustrine strata in the Baoshan Basin at the southeastern edge of the Tibetan Plateau. Geol. Bull. China 37, 759–775.
Qi, G., Dong, W., Zheng, L., Zhao, L., Gao, F., Yue, L., Zhang, Y., 2006. Taxonomy, age and environment status of the Yuanmou hominoids. Chinese Sci Bull 51, 704–712.
Raju, K.K., Ramprasad, T., Rao, P.S., Rao, B.R., Varghese, J., 2004. New insights into the tectonic evolution of the Andaman basin, Northeast Indian Ocean. Earth Planet. Sci. Lett. 221 (1–4), 145–162.
Replumaz, A., San Jose, M., Margirier, A., Beek, P., Gautheron, C., Leloup, P.H., Ou, X., Cao, K., Wang, G.C., Zhang, Y.Z., Valla, P.G., Balvay, M., 2020. Tectonic control on rapid late Miocene—quaternary incision of the Mekong River Knickzone, Southeast Tibetan Plateau. Tectonics 39 (2), e2019TC005782.
Roger, F., Calassou, S., Lancelot, J., Malavieille, J., Mattauer, M., Xu, Z.Q., Hao, Z.W., Hou, L.W., 1995. Miocene emplacement and deformation of the Konga-Shan granite (Xianshui he fault Zone, West Sichuan, China): geodynamic implications. Earth Planet. Sci. Lett. 130, 201–216.
Rohrmann, A., Kirby, E., Schwanghart, W., 2023. Accelerated Miocene incision along the Yangtze River driven by headward drainage basin expansion. Sci. Adv. 9, eadh1636.
Royden, L., Burchfiel, B.C., King, R.W., Wang, E., Chen, Z.L., Shen, F., Liu, Y.P., 1997. Surface deformation and lower crustal flow in eastern Tibet. Science 276, 788–790.
Schoenbohm, L., Burchfiel, B.C., Chen, L.Z., 2006a. Propagation of surface uplift, lower crustal flow, and Cenozoic tectonics of the southeast margin of the Tibetan Plateau. Geology 34, 813–816.
Schoenbohm, L., Burchfiel, B.C., Chen, L., Yin, J., 2006b. Miocene to present activity along the Red River fault, China, in the context of continental extrusion, upper-crustal rotation, and lower-crustal flow. Geol. Soc. Am. Bull. 118, 672–688.
Schoenbohm, L.M., Burchfiel, B.C., Liangzhong, C., Jiyun, Y., 2005. Exhumation of the Ailao Shan shear zone recorded by Cenozoic sedimentary rocks, Yunnan Province, China. Tectonics 24, TC6015.
Searle, M.P., Noble, S.R., Cottle, J.M., Waters, D.J., Mitchell, A.H.G., Hlaing, T., Horstwood, M.S.A., 2007. Tectonic evolution of the Mogok metamorphic belt, Burma (Myanmar) constrained by U-Th-Pb dating of metamorphic and magmatic rocks. Tectonics 26, TC3014.
Shen, X., Tian, Y., Li, D., Qin, S., Vermeesch, P., Schwanethal, J., 2016. Oligocene-early Miocene river incision near the first bend of the Yangtze River: Insights from apatite (U-Th-Sm)/He thermochronology. Tectonophysics 687, 223–231.
Shen, X., Tian, Y., Zhang, G., Zhang, S., Carter, A., Kohn, B., et al., 2019. Late Miocene hinterland crustal shortening in the Longmen Shan thrust belt, the eastern margin of the Tibetan Plateau. J. Geophys. Res. 124, 11,972–11,991.
Shen, X., Braun, J., Yuan, X., 2022. Southeastern margin of the Tibetan Plateau stopped expanding in the late Miocene. Earth Planet. Sci. Lett. 583, 117436.
Socquet, A., Pubellier, M., 2005. Cenozoic deformation in western Yunnan (China–Myanmar border). J. Asian Earth Sci. 24, 495–515.
Sorrel, P., Eymard, I., Leloup, P.H., Maheo, G., Olivier, N., Sterb, M., Gourbet, L., Wang, G., Jing, W., Lu, H., Li, H., Yadong, X., Zhang, K., Cao, K., Chevalier, M.L., Replumaz, A., 2017. Wet tropical climate in SE Tibet during the late Eocene. Sci. Rep. 7, 7809.

Spicer, R.A., Farnsworth, A., Su, T., 2020. Cenozoic topography, monsoons and biodiversity conservation within the Tibetan Region: An evolving story. Plant Divers. 42, 229–254.

Spurlin, M.S., Yin, A., Horton, B.K., Zhou, J., Wang, J., 2005. Structural evolution of the Yushu-Nangqian region and its relationship to syncollisional igneous activity east-Central Tibet. Geol. Soc. Am. Bull. 117, 1293–1317.

Studnicki-Gizbert, C., Burchfiel, B.C., Li, Z., Chen, Z., 2008. Early Tertiary Gonjo basin, eastern Tibet: sedimentary and structural record of the early history of India-Asia collision. Geos 4, 713–735.

Su, T., Wilf, P., Huang, Y.J., Zhang, S.T., Zhou, Z.K., 2015. Peaches preceded humans: fossil evidence from SW China. Sci. Rep. 5, 16794.

Su, T., Huang, Y.J., Meng, J., Zhang, S.T., Huang, J., Zhou, Z.K., 2016. A Miocene leaf fossil record of *Rosa (R. Fortuita n.* sp.*)* from its modern diversity center in SW China. Palaeoworld 25, 104–115.

Su, T., Spicer, R.A., Li, S.H., Xu, H., Huang, J., Sherlock, S., Huang, Y.J., Li, S.F., Wang, L., Jia, L.B., Deng, W.Y.D., Liu, J., Deng, C.L., Zhang, S.T., Valdes, P.J., Zhou, Z.K., 2019. Uplift, climate and biotic changes at the Eocene–Oligocene transition in south-eastern Tibet. Natl. Sci. Rev. 6, 495–504.

Sun, P.C., Li, C., Zhou, L., Qu, W., Wang, D., Gao, L., Li, W., Li, X., Zhao, H., Du, A., 2021. Dating metallogenic age of Jinding Pb-Zn deposit in Yunnan: evidence from Re-Os isotope of bitumen. Earth Sci. 46 (12), 4247–4259.

Sun, X., Tong, Y., Yang, Z., Pei, J., Pu, Z., Hou, L., Jin, S., Zhang, Z., Li, X., 2022. Magnetostratigraphic evidence from the Gengma Basin for the fast response of the crustal rotation of the northern part of the Shan-Thai Block to the India-Eurasia convergence. Geochem. Geophys. Geosyst. 23, e2022GC010556.

Tang, M., Liu-Zeng, J., Hoke, G.D., Xu, Q., Wang, W., Li, Z., Zhang, J., Wang, W., 2017. Paleoelevation reconstruction of the Paleocene-Eocene Gonjo basin, SE-central Tibet. Tectonophysics 712–713, 170–181.

Tao, J., Du, N., 1987. Miocene flora from Markam County and fossil record of Betulaceae. Acta Bot. Sin. 29, 649–655.

Tao, J., Kong, Z., 1973. The fossil florule and sporo-pollen assemblage of the Shang-in coal series of Eryuan, Yunnan. Acta Bot. Sin. 15 (1), 120–130.

Tao, Y., Zhang, H., Zhang, J., Pang, J., Wang, Y., Wu, Y., Zhao, X., Huang, F., Ma, Z., 2022. Late Cretaceous–Early Cenozoic exhumation across the Yalong thrust belt in eastern Tibet and its implications for outward plateau growth. Glob. Planet. Chang. 216, 103897.

Tapponnier, P., Peltzer, G., Le Dain, A.Y., Armijo, R., Cobbold, P., 1982. Propagating extrusion tectonics in Asia: new insights from simple experiments with plasticine. Geology 10, 611–616.

Tian, Y., Kohn, B.P., Gleadow, A.J.W., Hu, S., 2013. Constructing the Longmen Shan eastern Tibetan Plateau margin: Insights from low-temperature thermochronology. Tectonics 32, 576–592.

Tian, Y., Kohn, B.P., Hu, S., Gleadow, A.J.W., 2015. Synchronous fluvial response to surface uplift in the eastern Tibetan Plateau: Implications for crustal dynamics. Geophys. Res. Lett. 42, 29–35.

Tian, Y., Kohn, B.P., Phillips, D., Hu, S., Gleadow, A.J., Carter, A., 2016. Late Cretaceous–earliest Paleogene deformation in the Longmen Shan fold-and-thrust belt, eastern Tibetan Plateau margin: Pre-Cenozoic thickened crust? Tectonics 35 (10), 2293–2312.

Tian, Y., Spicer, R.A., Huang, J., Zhou, Z., Su, T., Widdowson, M., Jia, L., Li, S., Wu, W., Xue, L., Luo, P., Zhang, S., 2021. New early Oligocene zircon U–Pb dates for the 'Miocene' Wenshan Basin, Yunnan, China: Biodiversity and paleoenvironment. Earth Planet. Sci. Lett. 565, 116929.

Tian, Y., Liu, Y., Li, R., Sun, X., Zhang, Z., Carter, A., Vermeesch, P., 2022. Thermochronological constraints on Eocene deformation regime in the Long-Men Shan: Implications for the eastward growth of the Tibetan Plateau. Glob. Planet. Chang. 217, 103930.

Tian, Y.T., Kohn, B.P., Gleadow, A.J.W., Hu, S.B., 2014. A thermochronological perspective on the morphotectonic evolution of the southeastern Tibetan Plateau. J. Geophys. Res. 119, 676–698.

Tong, Y., Yang, Z., Pei, J., Wang, H., Wu, Z., Li, J., 2022. Upper crustal collapse reconstructed the topography and remodeled the fault system of the Chuandian fragment in the southeastern edge of the Tibetan plateau, evidenced by anisotropy of magnetic susceptibility data sets. Tectonics 41 (4), 2021TC007126.

Van Hinsbergen, D.J.J., Kapp, P., Dupont-Nivet, G., Lippert, P.C., DeCelles, P.G., Torsvik, T.H., 2011. Restoration of Cenozoic deformation in Asia and the size of Greater India. Tectonics 30, TC5003.

Wang, E., Burchfiel, B.C., 1997. Interpretation of Cenozoic tectonics in the right-lateral accommodation zone between the Ailao Shan shear zone and the eastern Himalayan Syntaxis. Int. Geol. Rev. 39, 191–219.

Wang, E., Burchfiel, B.C., Royden, L.H., Chen, L.Z., Chen, J.S., Li, W.X., Chen, Z.L., 1998. Late Cenozoic Xianshuihe-Xiaojiang, Red River, and Dali Fault Systems of Southwestern Sichuan and Central Yunnan, China. Geol. Soc. Am. Spec. Pap. 327, 1–108.

Wang, E., Kirby, E., Furlong, K.P., Van Soest, M., Xu, G., Shi, X., Kamp, P., Hodges, K., 2012. Two-phase growth of high topography in eastern Tibet during the Cenozoic. Nat. Geosci. 5 (9), 640–645.

Wang, G., Wan, J., Wang, E., Zheng, D., Li, F., 2008a. Late Cenozoic to recent transtensional deformation across the Southern part of the Gaoligong shear zone between the Indian plate and SE margin of the Tibetan plateau and its tectonic origin. Tectonophysics 460, 1–20.

Wang, H., Li, K., Tian, Y., Zhang, G., 2022a. Oligocene-early Miocene exhumation and shortening along the Anninghe fault in the southeastern Tibetan Plateau: insights from zircon and apatite (U-Th)/He thermochronology. Int. Geol. Rev. 64 (3), 390–404.

Wang, L., Yuan, Q., Shen, L., Ding, L., 2022b. Middle Eocene paleoenvironmental reconstruction in the Gonjo Basin, eastern Tibetan Plateau: evidence from palynological and evaporite records. Front. Earth Sci. 10, 818418.

Wang, S.F., Fan, C., Wang, G., Wang, E., 2008b. Late Cenozoic deformation along the northwestern continuation of the Xianshuihe fault system, Eastern Tibetan Plateau. Geol. Soc. Am. Bull. 120, 312–327.

Wang, W.M., 1996. A Palynological survey of Neogene strara in Xiaolongtan Basin, Yunnan Province of South China. Acta Bot. Sin. 38 (9), 743–748.

Wang, X., Metcalfe, I., Jian, P., He, L., Wang, C., 2000. The Jinshajiang–Ailaoshan Suture Zone, China: tectonostratigraphy, age and evolution. J. Asian Earth Sci. 18, 675–690.

Wei, H.H., Wang, E., Wu, G.L., Meng, K., 2016. No sedimentary records indicating southerly flow of the paleo-Upper Yangtze River from the first Bend in southeastern Tibet. Gondwana Res. 32, 93–104.

Woo, J.K., Han, D.F., Xu, Q.H., Lu, Q.W., Pan, Y.R., Zhang, X.Y., Zheng, L., Xiao, M.H., 1981. *Ramapithecus* skulls found first in the world-brief report on the excavation of the Lufeng fossil ape site in the winter of 1980. Sci. Bull. 11, 1018–1021.

Wu, F., Wan, B., Zhao, L., Xiao, W., Zhu, R., 2020. Tethyan geodynamics. Acta Petrol. Sin. 36, 1627–1674.

Wu, F., Fang, X., Yang, Y., Dupont-Nivet, G., Nie, J., Fluteau, F., Zhang, T., Han, W., 2022. Reorganization of Asian climate in relation to Tibetan Plateau uplift. Nat. Rev. Earth Environ. 3, 684–700.

Wu, J., Zhang, K., Xu, Y., Wang, G., Garzione, C.N., Eiler, J., Leloup, P.H., Sorrel, P., Mahéo, G., 2018. Paleoelevations in the Jianchuan Basin of the southeastern Tibetan Plateau based on stable isotope and pollen grain analyses. Palaeogeogr. Palaeoclimatol. Palaeoecol. 510, 93–108.

Xiang, H., Zhang, B., Zhang, W., Guo, S., Wan, J., 2009. Geological analysis and FT dating of crustal deformation in the Jianchuan basin since the Tertiary. Acta Geol. Sin. 83 (2), 230–238.

Xiao, R., Zheng, Y., Liu, X., Yang, Q., Liu, G., Xia, L., Bian, Z., Guan, J., Feng, P., Xu, H., Clift, P.D., Qiang, X., Zhang, Y., Zheng, H., 2021. Synchronous sedimentation in Gonjo Basin, Southeast Tibet in Response to India-Asia collision constrained by magnetostratigraphy. Geochem. Geophys. Geosyst. 22, e2020GC009411.

Xing, L., Lockley, M.G., Matsukawa, M., Klein, H., Zhang, J., Wang, T., Iv, W.S.P., Hu, J., Dai, H., Hu, H., 2018. Review and detailed description of sauropod-dominated trackways from the Upper cretaceous Jiangdihe Formation of Yunnan, China. Ichnos 26 (2), 108–118.

Xing, Y., Ree, R.H., 2017. Uplift-driven diversification in the Hengduan Mountains, a temperate biodiversity hotspot. Proc. Natl. Acad. Sci. USA 114, 3444–3451.

Xiong, J., Li, Y., Zhong, Y., Si, S., Yao, Y., 2016. Paleomagnetism of the Jianshui basin in Yunnan, SW China, and geomorphological evolution of the Yunnan Plateau since the Neogene. J. Asian Earth Sci. 123, 67–77.

Xiong, Z., Ding, L., Spicer, R.A., Farnsworth, A., Wang, X., Valdes, P.J., Su, T., Zhang, Q., Zhang, L., Cai, F., Wang, H., Li, Z., Song, P., Guo, X., Yue, Y., 2020. The early Eocene rise of the Gonjo Basin, SE Tibet: from low desert to high forest. Earth Planet. Sci. Lett. 543, 116312.

Xu, J., Ferguson, D.K., Li, C.S., Wang, Y.F., 2008. Late Miocene vegetation and climate of the Lühe region in Yunnan, southwestern China. Rev. Palaeobot. Palynol. 148, 36–59.

Xu, K., Kemp, D.B., Ren, J., Qian, W., 2023. Astronomically forced climate variability across the Eocene−Oligocene transition from a low latitude terrestrial record (Lühe Basin, South China). Geol. Soc. Am. Bull. 135, 2678–2690.

Xu, Q., 1992. The discovery of an early human ancestor and its signficance. In: China Cultural Relics Daily, July 2nd, 1992.

Yan, M., Zhang, D., Fang, X., Zhang, W., Song, C., Liu, C., Zan, J., Shen, M., 2021. New insights on the age of the Mengyejing formation in the Simao Basin, SE Tethyan domain and its geological implications. Sci. China Earth Sci. 64, 231–252.

Yan, Y., Carter, A., Huang, C.Y., Chan, L.S., Hu, X.Q., Lan, Q., 2012. Constraints on Cenozoic regional drainage evolution of SW China from the provenance of the Jianchuan Basin. Geochem. Geophys. Geosyst. 13, Q03001.

Yang, T.N., Liang, M.J., Fan, J.W., Shi, P.L., Zhang, H.R., Hou, Z.H., 2014. Paleogene sedimentation, volcanism, and deformation in eastern Tibet: Evidence from structures, geochemistry, and zircon U–Pb dating in the Jianchuan Basin, SW China. Gondwana Res. 26, 521–535.

Yuan, J., Yang, Z., Deng, C., Krijgsman, W., Hu, X., Li, S., Shen, Z., Qin, H., An, W., He, H., Ding, L., Guo, Z., Zhu, R., 2021. Rapid drift of the Tethyan Himalaya terrane before two-stage India-Asia collision. Natl. Sci. Rev. 8, 1–13.

Yue, L.P., Zhang, Y.X., Qi, G.Q., Heller, F.A., Wang, J.Q., Yang, L.R., Zhang, R., 2004. Paleomagnetic age and palaeobiological significance of hominoid fossil strata of Yuanmou Basin in Yunnan. Sci. China Ser. D 47, 405–411.

Yunnan Bureau of Geology and Mineral Resource (YBGMR), 1990. Regional Geology of Yunnan Province, pp. 1–726.

Zachos, J.C., Dickens, G.R., Zeebe, R.E., 2008. An early Cenozoic perspective on greenhouse warming and carbon-cycle dynamics. Nature 451, 279–283.

Zaw, K., 1990. Geological, petrological and geochemical characteristics of granitoid rocks in Burma: with special reference to the associated W-Sn mineralization and their tectonic setting. J. SE Asian Earth Sci. 4, 293–335.

Zhang, B., Yin, C.Y., Zhang, J.J., Wang, J.M., Zhong, D.L., Wang, Y., Lai, Q.Z., Yue, Y.H., Zhou, Q.Y., 2017. Midcrustal shearing and doming in a Cenozoic compressive setting along the Ailao Shan-Red River shear zone. Geochem. Geophys. Geosyst. 18 (1), 400–433.

Zhang, C., Guo, Z., Deng, C., Ji, X., Wu, H., Paterson, G.A., Chang, L., Li, Q., Wu, B., Zhu, R., 2016a. Clay mineralogy indicates a mildly warm and humid living environment for the Miocene hominoid from the Zhaotong Basin, Yunnan, China. Sci. Rep. 6, 20012.

Zhang, G., Tian, Y., Li, R., Shen, X., Zhang, Z., Sun, X., Chen, D., 2022. Progressive tectonic evolution from crustal shortening to mid-lower crustal expansion in the southeast Tibetan Plateau: a synthesis of structural and thermochronological insights. Earth Sci. Rev. 226, 103951.

Zhang, H., Oskin, M.E., Liu-Zeng, J., Zhang, P., Reiners, P.W., Xiao, P., 2016b. Pulsed exhumation of interior eastern Tibet: Implications for relief generation mechanisms and the origin of high-elevation planation surfaces. Earth Planet. Sci. Lett. 449, 176–185.

Zhang, W., Yan, M., Fang, X., Zhang, D., Zhang, T., Zan, J., Song, C., 2019. High-resolution paleomagnetic constraint on the oldest hominoid- fossil-bearing sequence in the Xiaolongtan Basin, southeast margin of the Tibetan Plateau and its geologic implications. Glob. Planet. Chang. 182, 103001.

Zhang, W., Fang, X., Zhang, T., Song, C., Yan, M., 2020. Eocene rotation of the northeastern central Tibetan Plateau indicating stepwise compressions and eastward extrusions. Geophys. Res. Lett. 47, e2020GL088989.

Zhang, X.Y., 1987. New materials of *Ramapithecus* from Keiyuan, Yunnan. Acta Anthropol. Sin. 2, 81–87.

Zhao, C., Xiong, Z., Farnsworth, A., Spicer, R.A., He, S., Wang, C., Deng, Z., Cai, F., Wang, H., Tian, X., Valdes, P., Lamu, C., Xie, J., Yue, Y., Ding, L., 2023. The late Eocene rise of SE Tibet formed an Asian 'Mediterranean'climate. Glob. Planet. Chang. 231, 104313.

Zheng, H., Clift, P.D., He, M., Bian, Z., Liu, G., Liu, X., Xia, L., Yang, Q., Jourdan, F., 2021. Formation of the first Bend in the late Eocene gave birth to the modern Yangtze River, China. Geology 49, 35–39.

Zheng, H., Yang, Q., Cao, S., Clift, P.D., He, M., Kano, A., Sakuma, A., Xu, H., Tada, R., Jourdan, F., 2022. From desert to monsoon: irreversible climatic transition at ~ 36 Ma in southeastern Tibetan Plateau. Progr. Earth Planet. Sci. 9, 12.

Zhou, Z., Liu, J., Chen, L., Spicer, R.A., Li, S., Huang, J., Zhang, S., Huang, Y., Jia, L., Hu, J., Su, T., 2022. Cenozoic plants from Tibet: an extraordinary decade of discovery, understanding and implications. Sci. China Earth Sci. 66 (2), 205–226.

Zhou, Z.K., 1985. The Miocene Xiaolongtan Fossil Flora in Kaiyuan, Yunnan, China. Ph. D. dissertation. Nanjing Institute of Geology and Palaeontology, Chinese Academy of Sciences, Nanjing.

Zhu, R., Potts, R., Pan, Y.X., Lue, L.Q., Yao, H.T., Deng, C.L., Qin, H.F., 2008a. Paleomagnetism of the Yuanmou Basin near the southeastern margin of the Tibetan Plateau and its constraints on late Neogene sedimentation and tectonic rotation. Earth Planet. Sci. Lett. 272, 97–104.

Zhu, R., Potts, R., Pan, Y.X., Yao, H.T., Lü, L.Q., Zhao, X., Gao, X., Chen, L.W., Gao, F., Deng, C.L., 2008b. Early evidence of the genus Homo in East Asia. J. Hum. Evol. 55, 1075–1085.

Zhu, R., Zhao, P., Zhao, L., 2021. Tectonic evolution and geodynamics of the Neo-Tethys Ocean. Sci. China Earth Sci. 65, 1–24.

Zhu, R.X., Liu, Q.S., Yao, H.T., Guo, Z.T., Deng, C.L., Pan, Y.X., Lü, L.Q., Chang, Z.G., Gao, F., 2005. Magnetostratigraphic dating of hominoid-bearing sediments at Zhupeng, Yuanmou Basin, southwestern China. Earth Planet. Sci. Lett. 236, 559–568.

Zong, G.F., Chen, W., Huang, X., Xu, Q., 1996. Cenozoic Mammals and Environment of Hengduan Mountains Region. China Ocean Press, Beijing.